1

1

2

3

4

5

6

7

8   **Review of aragonite and calcite crystal morphogenesis in thermal spring systems**

9   Brian Jones

10

11   Department of Earth and Atmospheric Sciences, University of Alberta, Edmonton, Alberta,

12   T6G 2E3, Canada.

13

14

15   Corresponding author E-mail: Brian.Jones@ualberta.ca

16

17   ABSTRACT

18   Aragonite and calcite crystals are the fundamental building blocks of calcareous thermal spring

19   deposits. The diverse array of crystal morphologies found in these deposits, which includes

20   monocrystals, mesocrystals, skeletal crystals, dendrites, and spherulites, are commonly

21   precipitated under far-from-equilibrium conditions. Such crystals form through both abiotic and

22   biotic processes. Many crystals develop through non-classical crystal growth models that

23   involves the arrangement of nanocrystals in a precisely controlled crystallographic register.

24   Calcite crystal morphogenesis has commonly been linked to a "driving force", which is a

25   conceptual measure of the distance of the growth conditions from equilibrium conditions.

26   Essentially, this scheme indicates that increasing levels of supersaturation and various other

27   parameters that produce a progressive change from monocrystals and mesocrystals to skeletal

28   crystals to crystallographic and non-crystallographic dendrites, to dumbbells, to spherulites.

29   Despite the vast amount of information available from laboratory experiments and natural spring

30   systems, the precise factors that control the driving force are open to debate. The fact that calcite

31   crystal morphogenesis is still poorly understood is largely a reflection of the complexity of the

32   factors that influence aragonite and calcite precipitation. Available information indicates that

33   variations in calcite crystal morphogenesis can be attributed to physical and chemical parameters

34   of the parent water, the presence of impurities, the addition of organic or inorganic additives to

35   the water, the rate of crystal growth, and/or the presence of microbes and their associated

36   biofilms. The problems in trying to relate crystal morphogenesis to specific environmental

37   parameters arise because it is generally impossible to disentangle the controlling factor(s) from

38   the vast array of potential parameters that may act alone or in unison with each other.

39   **Key words:** Calcite, aragonite, crystal morphogenesis, thermal springs, mesocrsystals

1. Introduction

40

41   Many thermal spring systems throughout the world (e.g., Waring, 1965; Pentecost, 2005),

42   are characterized by spectacular arrays of precipitates that are formed of amorphous calcium

43   carbonate, calcite, and aragonite. The development and appearance of these deposits is, to a

44   large extent, a reflection of (1) the precipitation of the different $CaCO_3$ polymorphs, and (2) the

45   calcite and aragonite crystal morphogenesis. Factors that control precipitation of the $CaCO_3$

46   polymorphs are outline in Jones (2017), whereas the calcite and aragonite crystal morphogenesis

47   is reviewed herein.

48   The calcite and aragonite crystals in spring deposits are commonly characterized by bizarre

49   morphologies that include single crystals of various morphologies, dendrite crystals, dumbbells,

50   fans, and spherulites (e.g., Folk et al., 1985; Guo and Riding, 1992; Jones and Renaut, 1995).

51   The fact that "…crystallization in natural environments rarely occurs near equilibrium"

52   (Fernández-Díaz et al., 1996, p. 482) means that it is commonly difficult to interpret and

53   understand the parameters that control calcite and aragonite crystal morphogenesis.

54   Interpretation of the unusual crystal morphologies found in spring systems using classical crystal

55   growth model, for example, is difficult and commonly yields conclusions that are open to debate.

56   Given the importance of $CaCO_3$ to materials science and chemical materials, laboratory

57   experiments have been routinely used to determine the factors that control calcite and aragonite

58   crystal morphogenesis. Collectively, these experiments have clearly illustrated that aragonite

59   and calcite precipitation is complex and controlled by many different parameters. Nevertheless,

60   these experiments have shown that crystal morphologies can be related to the types of hydrogels

61   used (Kulak et al., 2007; Meldrum and Cölfen, 2008; Song and Cölfen, 2010; Zhou et al., 2010;

62   Nindiyasari et al., 2015) as well as the organic and inorganic additives that are in the parent

63   solution (Sánchez-Pastor et al., 2011; Asenath-Smith et al., 2012; Dorvee et al., 2012;

64   Nindiyasari et al., 2014). Extracellular proteins and polysaccharides found in the

65   biomacromolecules, for example, play a major role in the precipitation of most $CaCO_3$

66   biominerals (e.g., Lowenstam and Weiner, 1989; Albeck et al., 1996; Belcher et al., 1996; Wang

67   et al., 2013). Laboratory analyses, like those conducted by materials scientists, provide

68   invaluable information that should be integrated with geological interpretations of precipitates

69   found in thermal spring systems.

70   With specific reference to deposits associated with thermal springs, the main purposes of

71   this review paper are to: (1) define the terminology that should be applied to aragonite and

72   calcite crystals, (2) determine if classical or non-classical crystal growth underpins aragonite and

73   calcite crystal growth, (3) discuss the factors that control aragonite and calcite crystal

74   morphogenesis, (4) determine the information that can be obtained from different crystal

75   morphologies, and (5) assess the importance of understanding crystal morphogenesis for

76   interpreting other parameters such as stable isotopes. Although this review shows that there is

77   considerable information available on the aragonite and calcite crystal morphogenesis in thermal

78   spring systems, it also demonstrates that precipitation is controlled by numerous interrelated

79   parameters that are extremely difficult to disentangle from each other.

80   **2. Crystal terminology**

81   A plethora of terms have been used to define and describe the myriad arrays of $CaCO_3$

82   crystals found in spring deposits. Further confusion arises when two or more terms have been

83   applied to crystals with identical morphologies. In other cases, commonly used terms appear to

84   have never been formally defined and are used under the assumption that everybody knows what

85   they mean. Given this situation, the terms that have been applied to $CaCO_3$ crystals are

86   reviewed, defined, and their validity and applicability assessed. In all cases, the definitions

87   adopted herein are based on morphological attributes and all are defined independent of genesis.

88   *2.1. Monocrystal*

89   Although the term monocrystal has long been used to describe a single crystal, no formal

90   definition has been used (e.g., Ramseier, 1967; Thattey and Risbud, 1969). Hence, Meldrum and

91   Cölfen (2008, p. 4335) defined a monocrystal as a "...crystalline solid in which the crystal lattice

92   of the entire sample is continuous and unbroken to the edge of the sample, with no grain

93   boundaries". The critical elements of this definition are that the lattice continues unbroken to the

94   crystal edges (Zhou and O'Brien, 2008), the packing of the unit cells is continuous, and the

95   macroscopic morphology is faceted (Imai, 2014).

96   *2.2. Porous monocrystal*

97   Zhou and O'Brien (2008) defined a porous monocrystal as a crystal with numerous internal

98   pores that range from a few nanometers to micrometers in size. Zhan et al. (2003) and Li and

99   Estroff (2007) also used this term to describe crystals that they grew in an agarose hydrogel. The

100 term "sponge crystal" has been applied to a monocrystal with "…continuous voids originating

101 from a series of neighboring vacancies…" (Inumaru, 2006, p. 157). It is, however, probably

102 easier to treat it as a porous crystal.

103 *2.3. Polycrystal*

104   A polycrystal, also known as a polcrystalline solid, is formed of random aggregates of

105 numerous grains/crystallites (Zhou and O'Brien, 2008; Imai, 2016).

106 *2.4. Mesocrystal*

107   Cölfen and Antonietti (2005, p. 5577) defined a mesocrystal as a "…superstructure of

108 crystalline nanoparticles with external crystal faces on the scale of some hundred nanometers to

109 micrometers….". Meldrum and Cölfen (2008, p. 4343), noting that mesocrystal is an

110 abbreviation for "mesoscopically structured crystal", defined it as a colloidal crystal that is

111 formed of nanocrystals that are "…aligned in common crystallographic register…. such that the

112 mesocrystal scatters X-rays or electrons like a single crystal and shows birefringence properties

113 of a single crystal". Since then, the term has been defined in many papers, but commonly with

114 subtle differences in the wording (Niederberger and Cölfen, 2006; Xu et al., 2006, 2008a, 2008b;

115 Zhou and O'Brien, 2008; Song and Cölfen, 2010; Seto et al., 2012; Zhou and O'Brien, 2012; Kim

116 et al., 2014; Bergström et al., 2015). Song and Cölfen (2010, p. 1301) noted that the

117 nanocrystals were of "…mesoscopic size (1-1000 nm)" and suggested that single crystals have a

118 coherence length of > 100 nm whereas the coherence length in mesocrystals is much smaller.

119 Imai (2016) also argued that the constituent nanocrystals should be < 1 μm long. Zhou and

120 O'Brien (2012, p. 620) suggested that the "Sole criterion for determining whether a material is a

121 mesocrystal or not is the unique crystallographically hierarchial structure, not its formation

122 mechanism". Kim et al. (2014) issued a note of caution by pointing out that the appearance of

123 mesocrystals can be misleading because nanocrystals evident on the surfaces may not be

124 representative of how the crystal actually grew.

125 *2.5. Mosaic crystals*

126   Also referred to as "mosaicism" and "mosaic structure", French and Koeberl (2010)

127 defined a mosaic crystal as a "…single uniform crystal that is formed of a large number of

128 smaller crystal domains (also called "subgrains") whose crystal lattices are slightly to

129 significantly misoriented to each other." Although Imai (2014, 2016) attributed this term to

130 Darwin (1922), the term "mosaic" was not used in that paper.

131   The definition does not carry any genetic connotations and has been used in many other

132 contexts, including shocked quartz crystals (Hörz and Quaide, 1973).

133 *2.6. Composite crystal, aggregate crystal, crystallites, and subcrystals*

134   In the geological literature, the terms composite or aggregate crystals have been used to

135 describe crystals formed of smaller units that have been labeled as crystallites or subcrystals

136 (e.g., Jones, 1989; Jones and Renaut, 1996b; Jones et al., 2005). These terms, however, do not

137 appear to have been formally defined. Wells and Bishop (1955) in describing amphiboles from

138 pegmatitic diorites on Jersey noted that "Only a small proportion of the amphiboles are

139 homogeneous single prisms: some are composite crystals built up of sub-individuals in parallel

140 growth." For calcite crystals, the terms "composite crystal" (Chafetz et al., 1985; Folk et al.,

141 1985, their p. 352; Given and Wilkinson, 1985, captions to their Figs. 2, 4; Sandberg, 1985,

142 caption to his Fig. 11) or "aggregate crystal" (Binkley et al., 1980, caption to their Fig. 2D-F;

143 Chafetz et al., 1985, caption to their Fig. 6; Taylor and Chafetz, 2004, captions for their Figs. 12-

144 14) have been used as descriptors for crystals that are formed of smaller units, typically with the

145 same external morphology, that have been referred to as "subcrystals" (Sandberg, 1985) or

146 "crystallites" (Binkley et al., 1980). Taylor and Chafetz (2004, caption for their Fig. 12) implied

147 that these terms were synonymous when they described an aggregate crystal formed of

148 "…hundreds of individual subcrystals (crystallites)….". In other cases, the smaller component

149 units have simply been described by their morphology (Chafetz et al., 1985; Given and

150 Wilkinson, 1985). Jones and Renaut (1996a), Jones et al. (2005), Jones and Peng (2014c) used

151   the term "composite crystal" for a crystal that was formed of smaller subcrystals (cf., Given and

152   Wilkinson, 1985; Sandberg, 1985).

153   With reference to non-geological crystals, Herbstein (2003, p. 303) stated that "*Composite*

154   crystals are formed by the ordered agglutination of crystals of the same or different types: a

155   presumed requirement is a close resemblance between the structures of the types." Desiraju

156   (2003, p. 466), however, suggested that a better term would be "cocrystal" because they are

157   "…two crystals that are joined together". A "composite crystal" has also been described as one

158   that contains "…at least two components, which have different unit cells within the same

159   crystal" (Coppens et al., 1990, p. 81).

160   Jones and Peng (2014a, 2014b, 2016b) abandoned these terms in favour of the terms

161   mesocrystals and nanocrystals as defined by Meldrum and Cölfen (2008). This definition is

162   maintained herein.

163   *2.7. Dendrite crystals*

164   Tschernoff (1879 – cited in Smith, 1965) first used the term "dendrite" to describe treelike

165   crystals (Doherty, 1980). Buckley (1951, his Fig. 1) and Strickland-Constable (1968, p. 287)

166   recognized numerous levels of branching in these crystals by using the terms primary branch (or

167   needle, stem), secondary branches, and tertiary branches. Although these crystals commonly

168   develop in one plane, three-dimensional forms are also known (Chalmers, 1964). If the spaces

169   between the branches are filled-in by calcite precipitation at a later stage, they are known as

170   "filled-in dendrites" (Buckley, 1951, p. 213). Lofgren (1974, his Table 2) also treated a dendritic

171   crystal as a "…tree-like single crystal" with the "…restriction that all branches of the dendrite be

172   part of a single crystal".

173   Although Keith and Padden (1964) did not use the term dendrite, they described crystals

174   that follow crystallographic or noncrystallographic branching patterns. Based on this, Jones and

175   Renaut (1995) introduced the concept of "crystallographic dendrites" and "noncrystallographic

176   dendrites". In the former, branching patterns follow crystallographic precepts whereas

177   noncrystallographic dendrites have branching patterns that do not conform to crystallographic

178   directions.

179   With the progressive documentation of calcite dendrites from many different hot-spring

180   systems throughout the world, it is becoming increasingly clear that these complex crystals are

181   characterized by many different morphologies. Although Jones and Renaut (1995) introduced

182   the terms "scandulitic dendrites" and "feather dendrites" as two specific types, this practise of

183   naming different morphological forms of dendrites has not continued (e.g., Jones and Peng,

184   2012). This can only be attempted once there is a better understanding of the full range of

185   morphologies associated with dendrite crystals.

186   *2.8. Skeletal crystals*

187   Lofgren (1974, his Table 2) defined a skeletal crystal as "Generally acicular crystals that

188   are incomplete. They often appear hollow in thin section or have irregular outlines that form

189   during crystal growth." Later, Alena et al. (1990, p. 539) used the term "sheath crystal" for

190   hollow columns/prisms. Jones and Renaut (1996b) used the term "skeletal crystal" in accord

191   with the definition offered by Lofgren (1974).

192   Gornitz and Schreiber (1981, p. 787) coined the term "skeletal halite cubes (hoppers)" with

193   the notion that skeletal crystals are "…those which develop branched, tree-like forms or hollow,

194   stepped depressions…". Southgate (1982, p. 393) used "skeletal hopper" for crystals with "…up

195   to six depressed or stepped crystal faces." Given that these crystals are not hollow, they do not

196   conform to the original definition of a skeletal crystal as proposed by Lofgren (1974).

197   Although Atanassova and Bonev (2006) used the term "skeletal-dendritic crystals" of

198   galena, they did not formally define the term. Their Figures 1 and 2, however, show crystals that

199   are akin to dendrite crystals as opposed to skeletal crystals as defined by Lofgren (1974).

200   *2.9. Dumbbell crystals*

201   The term "dumbbell crystal", also known as "wheat sheaf" or "sheaf of wheat" crystals

202   (Garcia-Ruiz, 1985; Dominguez Bella and Garcia-Ruiz, 1987; Chekroun et al., 2004) has been

203   used largely as a descriptor and there appears to no formal definition of the term. Fouke et al.

204   (2000, p. 573), however, described a dumbbell crystal as "…dumbbell-shaped aggregates

205   composed of parallel needles that spread at their ends into radiating bundles."

206   These crystals, which can be formed of aragonite or calcite, have also been divided into

207   "fuzzy dumbbells" (Folk, 1993) and "smooth dumbbells" (Buczynski and Chafetz, 1991).

208   *2.10. Spherulites*

209   This term has been used as a descriptor of spherical masses that are formed of radiating

210   needles (e.g., Folk, 1993). Similarly, Gránásy et al. (2005) described a spherulite as spherical

211   body with a "…densely branched polycrystalline solidification patterns…". They suggested that

212   a spherulite could (1) form directly by radially branching from a nucleus, or (2) involve two

213   stages whereby a "wheat-sheaf" developed first with the spaces between the terminal bulges

214   being filled-in at a later time.

215 **3. Classical versus non-classical crystal growth models**

216   The classical crystal growth model, in the simplest sense, involves an atom-by-atom

217 addition to a nucleus (Geng et al., 2010). Niederberger and Cölfen (2006) argued that the

218 primary building blocks like atoms, ions, or molecules initially form clusters that may attain the

219 size of a crystal nucleus before ion-by-ion attachment takes place and the unit cell replicates and

220 a crystal develops. In contrast, non-classical crystal growth is a particle-based reaction system

221 (Cölfen and Antonietti, 2005; Geng et al., 2010) that involves the development of mesocrystals

222 through "…the arrangement of primary nanoparticles into an iso-oriented crystal via oriented

223 attachment" (Niederberger and Cölfen, 2006, their Fig. 1). Subsequent fusion of the

224 nanoparticles produces a monocrystal (Niederberger and Cölfen, 2006). The notion of non-

225 classical crystal growth arose from the experimental precipitation of titania (TiO_2) by Penn and

226 Banfield (1998a, 1998b, 1999). Although Penn and Banfield (1999) acknowledged that classical

227 crystal growth takes place, they also described a second mechanism of crystal growth whereby

228 solid particles were attached to a crystal surface in a precisely controlled crystallographic

229 manner. Penn and Banfield (1998a, p. 969) argued that this "oriented attachment" involved the

230 "…spontaneous self-organization of adjacent particles so that they share a common

231 crystallographic orientation, followed by joining of these particles to a planar interface". Since

232 then, many studies have demonstrated that the "oriented attachment mechanism" is common in

233 the growth of many crystals of various compositions, including the three $CaCO_3$ polymorphs

234 (Zhang et al., 2010, their Table 1). Song and Cölfen (2010) argued that alignment of the

235 nanocrystals might be controlled by (1) a structured organic matrix with oriented compartments

236 that became filled with crystalline matter, or promoted particle alignment, (2) physical fields or

237 mutual alignment of crystal faces, (3) epitaxial growth with mineral bridging connecting the

238 constituent nanocrystals, and/or (4) alignment of the nanocrystals by spiral constraints.

239 **4. Crystal morphologies in thermal spring deposits**

240   Aragonite and calcite, which are the two main $CaCO_3$ polymorphs found in thermal spring

241 deposits, are characterized by many different crystal morphologies (Fig. 1). The diversity of

242 aragonite crystals is, however, far less than that associated with the calcite.

243 *4.1. Aragonite crystal morphologies*

244   Aragonite crystals, which are typically elongate prisms with hexagonal cross-sections, have

245 been documented from many springs, including those in the Kenya Rift Valley (Jones and

246 Renaut, 1996a, their Figs. 5, 6), China (Jones and Peng, 2014a, their Fig. 6; 2014c, their Fig. 4;

247 2016b, their Fig. 8), Italy (Guo and Riding, 1992, their Figs. 6-8; Folk, 1994, his Figs. 8-11), and

248 Japan (Okumura et al., 2011; Okumura et al., 2012). Cyclic twinning (Fig. 2A) appears to be a

249 characteristic trait of many of these aragonite crystals (Jones and Renaut, 1996a, their Fig. 7A-E;

250 Jones and Peng, 2014c, their Fig. 6B; 2014a, their Fig. 4A-C; 2016b, their Fig. 8C).

251   Aragonite crystals in spring precipitates are commonly arranged in (1) bushes (Fig. 2B), (2)

252 dumbbells (Fig. 2C), and (3) spherical arrays (Fig. 2D). Although the bushes are characterized

253 by branching, they do not appear to be true dendrites (Fig. 2B). Each "branch" in the aragonite

254 bushes found in spring deposits at Jifei (Yunnan Province, China), for example, is a single

255 crystal that radiates outwards from common nucleation centres (Jones and Peng, 2014a).

256 *4.2. Calcite crystal morphologies*

257   Oaki and Imai (2003, their Fig. 1) broadly divided crystals into "single crystals"

258 (monocrystals) and "polycrystals". For convenience, this division is used herein for the purpose

259   of describing the morphologically diverse array of calcite crystals found in spring deposits (Fig.

260   1).

261   *4.2.1. Monocrystals*

262   Included in this general category are monocrystals, porous monocrystals, mesocrystals,

263   mosaic crystals, and skeletal crystals (Figs. 3-5). Although commonly formed of nanocrystals,

264   these crystals do not branch.

265   Mesocrystals have been documented from many spring deposits, including Big Hills

266   Spring, Canada (Turner and Jones, 2005, their Figs. 6, 7, 8A), Fall Creek, Canada (Rainey and

267   Jones, 2007, their Fig. 3), Clinton, Canada (Jones and Renaut, 2008, their Fig. 9H), Shuzhishi,

268   China (Jones and Peng, 2012, their Figs. 9G-M, 10), Jifei, China (Jones and Peng, 2014a, their

269   Fig. 12I, K), LaXin, China (Jones and Peng, 2014c, their Figs. 4K, L, 5B, C, F), and Shiqiang,

270   China (Jones and Peng, 2016b, their Fig. 10). Mesocrystals have also been produced in

271   experiments that model spring systems (Rogerson et al., 2008, their Fig. 2E; Pedley et al., 2009,

272   their Fig. 7C). Water temperature does not appear to be a controlling factor because the above

273   list of examples includes a range from cold (Big Hills Spring at ~ 7°C) to hot (e.g., LaXin at

274   100°C) springs.

275   Spectacular examples of calcite mesocrystals are common in precipitates from an unnamed

276   spring at Lýsuhóll, Iceland (Fig. 3) where the water temperature ranges from 20°C at the vent to

277   16°C on the distal edge of the discharge apron, which is ~ 6 m from the vent. Mesocrystals

278   found ~ 3 m from the vent are formed of numerous aligned nanocrystals that are each ~ 1.6 x 1.1

279   x 0.2 μm (Fig. 3A). Each nanocrystal, however, is formed of even smaller units that are of

280   variable size, ranging from 100 nm x 90 nm x 50 nm to 250 nm x 200 nm x 100 nm (Fig. 3B-E).

281   Irrespective of size, all of these smaller units have the same alignment and they are evident on all

282 faces of the mesocrystal (Fig. 3A-C). In another sample from the same area, the prismatic calcite

283 crystals (Fig. 3F) are also formed of perfectly aligned nanocrystals (Fig. 3F-I). Many of these

284 nanocrystals, however, are incompletely formed and commonly appear to be porous (Fig. 3H, I).

285   Not all mesocrystals display a perfect external form. Many calcite dodecahedra, which are

286 characterized by 12 pentagonal faces, are characterized by beveled edges that result from

287 incomplete growth of the crystal faces (Fig. 4). In spring deposits in Yunnan Province, China

288 (Jones and Peng, 2014c, 2014a, 2016b), these types of crystals are locally common and typically

289 are not attached to a substrate (Fig. 4A). Such clusters usually include crystals of various sizes

290 and variable development (Fig. 4B, C). Thus, some have poorly developed crystal faces and

291 edges (Fig. 4B), whereas others have better developed faces and some have sharply defined

292 crystal edges (Fig. 4C). Irrespective of their morphology, these crystals are formed of

293 nanocrystals (Fig. 4B, C). At Jifei, a PVC pipe that transported spring water from one site to

294 another became lined with calcite after six months (Jones and Peng, 2014a). Those precipitates

295 included dodecahedrons that, like the crystals in the spring deposits, are of variable size and

296 development (Fig. 4D, E). The crystal faces, where developed, are smooth and display no

297 clearly defined nanocrystals (Fig. 4D). In areas where the crystal faces are not developed,

298 however, nanocrystals are apparent in the interior (Fig. 4E). Dodecahedrons in spring deposits at

299 LaXin (Jones and Peng, 2014c) range from almost perfectly formed crystals (Fig. 4F), to crystals

300 that are clearly formed of nanocrystals, to those formed of nanocrystals but with poorly

301 developed smooth crystal faces (Fig. 4G-I). In the latter case, the crystal faces appear to start

302 growth from a central position and then spread laterally (Fig. 4H). During their initial stages of

303 development, the faces are ovoid with no evidence of sharp crystal edges (Fig. 4I).

304   Prismatic trigonal calcite mesocrystals are one of the most common types of mesocrystals

305   found in spring systems. They are, for example, important components of the "lily-pads" found

306   along the margins of one of the pools in the Waikite Spring system, New Zealand (Fig. 5A-F)

307   where the water temperature is 95-100°C (Jones and Renaut, 1996b) and from an old, inactive

308   cool-water spring system near Clinton, British Columbia, Canada (Jones and Renaut, 2008). In

309   samples from Waikite, the trigonal prismatic calcite crystals are formed of trigonal nanocrystals

310   that are aligned in the same crystallographic register (Fig. 5A-F). All of these mesocrystals are

311   porous with the size and shape of the internal pores defined by the packing of the nanocrystals

312   (Fig. 5B, C). Some prisms are skeletal with walls, formed of aligned trigonal nanocrystals, that

313   are arranged around the hollow core (Fig. 5D, F). In spring deposits from Clinton, there are

314   numerous examples of trigonal prismatic crystals formed of trigonal prismatic nanocrystals (Fig.

315   5G-I).

316   Collectively, these examples demonstrate that rhombic, trigonal, and dodecahedral

317   mesocrystals (Fig. 3-5) are common components of many spring deposits. In this context, it is

318   important to note that similar crystal morphologies are evident from geographically disparate

319   springs that are commonly characterized by vastly different environmental regimes. The fact

320   that mesocrystals have not been recorded from every spring deposit can probably be attributed to

321   (1) most precipitates not being examined on the SEM at the high magnifications required for

322   their recognition, (2) masking of the nanocrystals by fusion, (3) the fact that crystal growth did

323   not involve the systematic attachment of nanocrystals to the crystal growth surfaces, and/or (4)

324   miscommunications because of the lack of uniform terminology to describe these complex

325   crystal forms.

326   *4.2.2. Polycrystals*

327   The branching crystals in this general category include crystallographic dendrites, non-

328   crystallographic dendrites, dumbbells, and spherulites (Fig. 1).

329   Dendritic calcite crystals (Figs. 6, 7) are common components of many spring deposits

330   associated with waters of all temperatures throughout the world (Jones et al., 2000; Turner and

331   Jones, 2005; Jones and Renaut, 2008; Rainey and Jones, 2009). These three-dimensional

332   crystallographic and non-crystallographic crystals, which can be up to 12 cm long, are

333   morphologically variable and attempts to find dendrite crystals with similar morphologies from

334   different springs have been largely futile. At any given locality, however, the morphology and

335   structures of the calcite dendrites tends to be relatively constant. In old spring deposits near

336   Clinton (Jones and Renaut, 2008), the dendrites are built of small crystals that are nested and

337   stacked so that branches with relatively consistent architecture have developed (Fig. 7A, B).

338   SEM imaging shows that most of these crystals are incompletely formed and possibly skeletal

339   (Jones and Renaut, 2008, their Fig. 5). Large dendrites found in a riverside exposure at

340   Shuzhishi (Rehai geothermal area, Tengchong, China), which are up to 6 cm high and 3 cm in

341   diameter (Fig. 7C, D), have a completely different architecture from those at Clinton. Those

342   dendrites, which have a consistent architecture throughout the exposure, are bush-like with

343   numerous levels of branches that all developed through crystal splitting (Fig. 7C, D).

344   Comparison of these dendrites with those found in other springs like those at Lake Bogoria,

345   Kenya (Jones and Renaut, 1995), Waikite hot springs, New Zealand (Jones et al., 2000), and

346   Lýsuhoóll, Iceland (Jones et al., 2005), further underlines the fact that dendrites tend to be

347   morphological consistent at a given locality but incredibly variable from locality to locality.

348   Dumbbells (Fig. 8E) and spherulitic arrays (Fig. 1F) are formed of calcite or aragonite

349   crystals that radiate from a central point. Examples of dumbbells are known from many springs

350   including those in the USA (Chafetz et al., 1991, their Fig. 12F) and Italy (Guo and Riding,

351   1992, their Fig. 6A, B).

352   **5. Crystal morphogenesis**

353   *5.1. Experimental approach*

354   Fisher and Simons (1926) and McCauley and Roy (1974) were among the first to

355   experimentally grow calcite crystals in gels, and Devery and Ehlmann (1981) subsequently used

356   experimental data to suggest that the crystal form of calcite progressively changed as the Mg

357   content increased. Since then, the importance of $CaCO_3$ to materials science and chemical

358   materials has triggered numerous experimental studies for examining the parameters that control

359   crystal morphogenesis (e.g., Meldrum, 2003; Meldrum and Cölfen, 2008; Song et al., 2009; Song

360   and Cölfen, 2011; Sand et al., 2012). Collectively, these experiments are characterized by an

361   incredible diversity of the substances used and experimental conditions. Gehrke et al. (2005, p.

362   1317), for example, noted that they include (1) fast stopped flow techniques with crystallization

363   taking place within milliseconds, (2) slow gas diffusion methods, and (3) vapor diffusion

364   methods whereby thermal decomposition of ammonium carbonate allows for the slow generation

365   of CO_2. Some experiments are inorganic with patterns of crystallization being linked to

366   additives such as Mg (e.g., Reddy and Nancollas, 1976; Reddy and Wang, 1980; Meldrum and

367   Hyde, 2001), Li (Meldrum, 2003), or Sr (Reddy and Nancollas, 1976). Other experiments use

368   organic macromolecules like chitin or collagen (Song and Cölfen, 2011) in an attempt to mimic

369   the development of biogenic $CaCO_3$. Although solution-based, many experiments also utilize

370   aragose, silica, or gelatin hydrogels (e.g., Nindiyasari et al., 2015) to model precipitation in

371   organic templates like those associated with echinoids and other animals.

372   The concept of mesocrystals that develop by non-classical crystal growth mechanisms has

373   been largely underpinned by the desire to understand how various invertebrate animals control

374   precipitation of their calcareous skeletons (e.g., Zhou et al., 2009; Wang et al., 2013; Bergström

375   et al., 2015). These concepts, however, are also applicable to other geological environments,

376   include spring systems, where biofilms are common and play a significant role in the

377   precipitation of $CaCO_3$ (e.g., Jones and Peng, 2014c). In addition, the growth of crystals under

378   laboratory conditions has also led to over-arching concepts that try to explain how and why

379   different crystal morphologies are related (e.g., Sunagawa, 1981, 1982).

380   Sunagawa (1981, his Fig. 2; 1982) argued that with increasing supersaturation levels in the

381   parent fluid, crystal morphology changes from polygonal to hopper to dendrite to spherulitic.

382   Oaki and Imai (2003, their Fig. 1), based entirely on laboratory experiments, related a spectrum

383   of crystal forms to a "driving force" (Fig. 8) that Imai et al. (2006, their Fig. 1) later related to the

384   "distance from equilibrium". Oaki and Imai (2003) argued that crystal morphology depended on

385   various parameters including the density of the gel matrix used in the experiments. Thus, Imai

386   (2016, his Fig. 6) specifically related the progressive change in crystal morphologies to the

387   density of the gel matrix in which the crystals had been grown (Fig. 8). Oaki and Imai (2003)

388   and Imai (2016) argued that kinetic parameters controlled monocrystal development, whereas

389   diffusion was largely responsible for the more complex crystals at the higher end of the spectrum

390   (Fig. 8). Sunagawa (2005) also suggested that the progressive change from monocrystals to

391   hopper crystals to dendrites to polycrystalline forms was related to a "driving force" that was

392   primarily related to supersaturation levels. This scheme was later adopted by Beck and

393   Andreassen (2010, their Fig. 6).

394   Overall, the precipitation of aragonite crystals seems to have received far less attention than

395   the precipitation of calcite crystals. Zhou et al. (2009, their Figs. 1-5), however, produced

396   hexagonal aragonite mesocrystals with readily apparent nanocrystals. Although single crystals

397   were the most common, these experiments also produced dumbbells (Zhou et al., 2009, their Fig.

398   5c, d).

399   *5.2. Field-based approach*

400   Prismatic hexagonal crystals characterized by cyclical twinning (Fig. 2A) seems to the

401   most common morphology of aragonite found in thermal spring deposits. Variance in the

402   aragonite precipitates arises largely from crystal size and the manner in which the aragonite

403   crystals are arranged relative to each other. In many spring deposits, small needle-like aragonite

404   crystals collectively form bushes (Fig. 2B), fans and dumbbells (Fig. 2C), or spheres (Fig. 2D).

405   Although aragonite crystals in thermal spring deposits are commonly < 1 mm long, crystals up to

406   4 cm long and 4 mm wide are known from some of the springs in the Kenyan Rift Valley (Jones

407   and Renaut, 1996a).

408   Based on their assessment of calcite crystals found in spring deposits in the Kenyan Rift

409   Valley, Jones and Renaut (1995, their Fig. 14) argued that crystal morphology was related to a

410   "driving force" that included parameters such as supersaturation and supercooling. They used

411   the term "driving force" used because it was impossible to identify the precise factor(s) that had

412   triggered precipitation and determined crystal morphology. Changes in the driving force

413   produced a spectrum of crystal morphologies that ranged from skeletal crystals to

414   crystallographic dendrites to noncrystallographic dendrites to spherulitic crystals (Fig. 1). In the

415   context of this scheme, the monocrystals, mesocrystals, mosaic crystals, and porous crystals are

416   at the low end of the spectrum (Fig. 1). The scheme proposed by Jones and Renaut (1995, their

417   Fig. 14) includes elements found in the schemes produced by Sunagawa (1981, his Fig. 2) and is

418   very similar to the sequence of Oaki and Imai (2003, their Fig. 1) and subsequently modified by

419   Imai (2016, his Fig. 7a).

420   The calcite mesocrystals shown in Figures 2-5 are formed of oriented aggregates like the

421   nanocrystals that are evident in many laboratory-produced mesocrystals (e.g., Cölfen and

422   Antonietti, 2005, their Fig. 17; Kulak et al., 2007, their Figs. 2-5; Helbig, 2008, his Fig. 5;

423   Meldrum and Cölfen, 2008, their Fig. 68; Song and Cölfen, 2010, their Fig. 2; Zhou et al., 2010,

424   their Figs. 7, 8; Imai, 2016, his Fig. 8). Although the nanocrystals in most laboratory-produced

425   mesocrystals are of relatively uniform size, this is not universally true for natural mesocrystals

426   found in thermal spring deposits. The nanocrystals evident in the tabular mesocrystals from

427   Lýsuhóll, for example, are of uniform morphology but variable size (Fig. 3A-E). Similarly, in

428   some of these natural examples, some of the nanocrystals are incompletely formed (Fig. 3H, I).

429   Despite these morphological variations, all of the nanocrystals have a common crystallographic

430   register. Irrespective of these nuances, it is readily apparent that calcite mesocrystals are

431   common in many spring systems and that non-classical crystal growth is operative.

432   **6. Integration of data from experimental and natural aragonite and calcite crystals**

433   Ideally, it should be possible to gain a better understanding of the processes that control

434   aragonite and calcite crystal morphogenesis by merging the information derived from laboratory

435   experiments with that derived from natural crystals. Unfortunately, there are inherent problems

436   with each approach and it is commonly difficult to merge the two types of data in a meaningful

437   way. In part, this is due to the inherent problems associated with each method of analysis.

438   *6.1. Problems with data from experimental approach*

439   When considered in the content of natural spring systems, the following problems arise

440   with respect to information obtained from laboratory experiments.

441   • The number of variables associated with laboratory experiments are much lower than in

442   natural systems. Thus, there is no assurance that a variable deemed responsible for a

443   specific crystal morphology in the laboratory experiment will have the same affect in

444   natural systems where the number of variables and inter-relationships between variables are

445   much higher.

446   • Laboratory experiments are typically of short duration (hours to weeks) and therefore

447   contrast sharply with the long periods over which most modern springs have been

448   operative.

449   • Many laboratory experiments are run at room temperature (typically $\sim 25°C$) and therefore

450   may not be good models for thermal springs, where water temperature may be up to $100°C$.

451   • Many laboratory experiments are abiogenic and hence difficult to apply to natural spring

452   systems where microbes and biofilms are common.

453   *6.2. Problems with data from natural spring systems*

454   In modern active springs, critical issues that arise in assessing the factors that control

455   crystal morphogenesis includes the following.

456   • In many studies, there has been an inherent assumption that the classical crystal growth

457   model underpins all precipitation in spring systems. Hence, the possibility that non-

458   classical crystal growth mechanisms were operative has been ignored.

459   • Any attempt to link crystal morphogenesis to specific attribute(s) of the spring water

460   implicitly assumes that the modern spring waters were responsible for their precipitation.

461   This may not always be true because short-term temporal changes in the composition of

462   spring waters are common in many springs. For Dagunguo hot spring in the Tengchong

463   area (China), for example, the percentage of CO_2 in the gases varied from 49.7 to 99.7%

464   between 1980 and 2000 (Du et al., 2005, their Table 4). Changes like these, also known in

465   other springs in Yunnan and Sichuan provinces, can be triggered by earthquakes (Ren et

466   al., 2005), hydrothermal explosions (Shangguan et al., 2005), and time variable

467   contributions of CO_2 from different sources (Du et al., 2005). Although the example of

468   Dagunguo involves the CO_2 levels, similar changes in other components of the spring

469   water can also occur over short time periods.

470   • In many cases, linking crystal morphogenesis to specific physical (e.g., water T) or

471   chemical (e.g., Mg content) attributes of the spring water tacitly assumes that the process is

472   inorganic. The presence of organic macromolecules or microbial mats in the spring system

473   may, however, have a significant impact on the processes that govern precipitation and

474   crystal morphogenesis.

475   • Given that many aragonite and calcite crystals in modern springs are typically very small

476   (commonly < 1 mm), it is virtually impossible to actively monitor the microenvironment

477   around a growing crystal. This is especially true if the crystals are growing in the biofilms

478   generated by the microbes, which are typically characterized by microdomians that are < 1

479   μm long (Peng and Jones, 2013).

480 **8. Discussion**

481   In the broadest sense, precipitation of aragonite and calcite in laboratory experiments and

482 natural spring systems is a three-phase system involving water, organic molecules, and solids

483 (e.g., Sand et al., 2012). Each of these end members, however, encompass numerous parameters

484 that can influence crystal morphogenesis. Important aspects of the water, for example, include

485 temperature, pH, dissolved elements (e.g., Ca, Mg, Sr), and associated gases (e.g., CO_2).

486 Likewise, the organic component varies in terms of its density, porosity, composition, and the

487 physical and biochemical characteristics. Collectively, this means that the degrees of freedom

488 associated with these systems is very high.

489 The driving force of crystallization can, in its simplest sense, be equated to the degree of

490 supersaturation of the fluid with respect to $CaCO_3$ (e.g., Torrent-Burgués, 1994; Ruiz-Agudo et

491 al., 2011). The driving force of crystallization is, however, a thermodynamic measure and in

492 itself, cannot always explain precipitation because kinetic factors (Torrent-Burgués, 1994) and

493 other variables such as the Ca^{2+} to CO_3^{2-} ratio (Ruiz-Agudo et al., 2011; Van der Weijden and

494 Van der Weijden, 2014), pH (Ruiz-Agudo et al., 2011), and/or Mg content (Wasylenki et al.,

495 2005) can influence $CaCO_3$ precipitation and crystal growth. As yet, it has proven impossible to

496 disentangle these parameters so that the prime controller of precipitation and crystal

497 morphogenesis can be clearly identified. As a result, the "driving force", which is a key element

498 of the crystal growth schemes defined by Jones and Renaut (1995), Oaki and Imai (2003), Imai

499 et al. (2006), Imai and Oaki (2010), and Imai (2014) is a conceptual magnitude that includes all

500 of the parameters that control $CaCO_3$ precipitation and crystal morphogenesis. The complexity

501 of the system has been clearly demonstrated by the inorganic experimental precipitation of

502 aragonite and calcite whereby different crystal morphologies are produced by adjusting

503 parameters such as temperature and Mg content (e.g., Reddy and Nancollas, 1976; Loste et al.,

504 2003; Meldrum, 2003; Song and Cölfen, 2011). Similarly, experimental modeling of organic

505 systems has shown that variations in hydrogel attributes (e.g., porosity) can play a critical role in

506 crystal morphogenesis (e.g., Oaki and Imai, 2003; Nindiyasari et al., 2014, 2015; Imai, 2016).

507 Nindiyasari et al. (2014), for example, experimentally demonstrated that the solid content of the

508 gelatin hydrogel influenced crystal morphology because it caused changes in the diffusivity that,

509 in turn, controlled the volume of aqueous solution so that the classic layer-by-layer growth of

510 crystals changed to the aggregate mechanism that produced mesocrystals.

511 Imai et al. (2006, their Fig. 1) argued that crystal growth is fundamentally controlled by the

512 "distance from equilibrium", which they defined as the difference between the growth conditions

513 and the equilibrium state. Oaki and Imai (2003), Kulak et al. (2007), and Imai (2014) suggested

514 that euhedral crystals form largely by kinetic-controlled reactions in near-equilibrium conditions

515 whereas dendritic and spherulitic crystal growth takes place in far-from-equilibrium conditions.

516 Critically, as the driving force increases, the crystal growth rate becomes increasingly controlled

517 by diffusion or heat transfer (Imai et al., 2006).

518 In the context of natural spring systems, resolution of the factor(s) that control aragonite

519 and calcite crystal morphologies must determine the factor(s) that contribute to the driving force,

520 or more precisely the distance between the growth conditions and equilibrium conditions (cf.,

521 Imai et al., 2006). A critical decision in this respect is whether or not inorganic or organic

522 precipitation was operative and specifically if microbes and biofilms were involved. Such an

523 assessment is not always straightforward in natural systems because the presence of

524 biofilms/microbes relies largely on physical evidence of their presence. Although commonly

525 well-preserved in opal-A precipitates found in spring systems (e.g., Oehler and Schopf, 1971;

526 Francis et al., 1978; Westall et al., 1995; Cady and Farmer, 1996; Jones et al., 1998, 2003;

527 Renaut et al., 1998; Konhauser et al., 1999), microbes are rarely preserved in aragonite or calcite

528 precipitated around thermal springs (Jones and Renaut, 1995; Peng and Jones, 2012). Likewise,

529 extracellular polymeric substances (EPS) are rarely calcified and evidence of their presence in

530   older deposits is sparse. Substrates in one spring at Lýsuhóll, Iceland, where calcite crystals are

531   being precipitated, for example, are covered with thriving biofilms (Fig. 6). Although biofilms

532   are obvious in the field, samples of the calcite mesocrystals collected from this spring do not

533   contain any calcified microbes and isolated strands of EPS offer the only evidence of microbial

534   involvement (Fig. 3A-C, F). Likewise, no mineralized microbes or EPS are associated with the

535   dodecahedrons shown in Figure 4 and the dendrites shown in Figure 7. Thus, even in these

536   young, relatively fresh samples, the lack of preserved EPS or mineralized microbes means that

537   there is little or no direct evidence of microbial involvement in the calcite/aragonite precipitation.

538   With the passage of time and diagenesis, any traces of microbes or EPS would be rapidly lost.

539   Thus, in older spring deposits the evidence would typically indicate that microbes played a

540   minimal role in their formation (e.g., Jones et al., 2004). Evidence for the presence of biofilms

541   and/or microbes may, however, come from the crystals themselves. Numerous experiments have

542   shown, for example, that mesocrystals commonly develop when precipitation takes place in

543   hydrogel media (e.g., Niederberger and Cölfen, 2006; Nindiyasari et al., 2014, 2015), which can

544   be viewed as the laboratory equivalents of the biofilms found in spring systems.

545   One of the most intriguing aspects of $CaCO_3$ crystal morphogenesis is the contrast between

546   the arrays of aragonite and calcite crystal forms that are commonly associated with spring

547   deposits. Aragonite crystals display limited morphologically variability, with most being

548   cyclically twinned hexagonal prisms with pointed termini (Jones and Renaut, 1996a), which have

549   been found in many geographically disparate hot spring deposits. Variations in the aragonite

550   precipitates comes from the assembly of these crystals into bushes (Fig. 2B), radiating fans, or

551   spherulites (Fig. 2C, D). In contrast, calcite is characterized by an amazing array of different

552   crystal forms that range from rhombic mesocrystals (Fig. 3), to skeletal crystals, to trigonal

553   mesocrystals (Fig. 5), to dodecahedrons (Fig. 4), to various types of complex dendrites (Fig. 7).

554   Although the reason(s) for the contrast in crystal diversity between the two polymorphs is not

555   known, it may be rooted in the fact that aragonite and calcite belong to two different crystal

556   systems.

557   Some of the most extreme crystal morphologies develop when the crystal growth

558   environment is far-from-equilibrium (Figs. 1, 8). This situation commonly arises where there is

559   rapid CO_2 degassing from spring waters, especially in situations where the spring waters are

560   supercharged with CO_2 that may have been derived from the mantle, magmatic bodies, and/or

561   sedimentary carbonates. In this context, two aspects are important, namely (1) CO_2 is commonly

562   the dominant gas associated with thermal springs (commonly > 90% of total gases, by volume)

563   in the Tenchong volcanic area (Du et al., 2005, their Table 4) and the Kenya Rift Valley

564   (McCall, 1967; Darling et al., 1995), and (2) the CO_2 content is known to vary with time; for

565   example, in Yunnan and Sichuan provinces of China, the CO_2 varies in accord with earthquake

566   activity (Ren et al., 2005), hydrothermal explosions (Shangguan et al., 2005), and temporal

567   variations related to the CO_2 source (Du et al., 2005). Although CO_2 degassing has been

568   commonly been linked to the $CaCO_3$ polymorph that is precipitated in a given system (Kitano,

569   1962), relatively little is known about its influence on crystal morphogenesis. Nevertheless,

570   crystal morphologies indicative of far-from-equilibrium precipitation (Figs. 1, 8) are common in

571   springs where CO_2 degassing is known or inferred to be high based on independent evidence

572   (e.g., Renaut and Jones, 1997; Jones and Peng, 2012, 2016b). In some spring systems, it appears

573   that precipitation of dendrites and other complex morphologies is not continuous but possibly the

574   result of episodic variations in some aspect of the spring water chemistry. As noted previously,

575   temporal variations in CO_2 emissions from springs are known and is therefore possible that they

576   may be the cause of such precipitation.

577   Although dendritic and spherulitic crystal growth has commonly been linked to high

578   supersaturation levels, it has also been argued that the addition of impurities may be responsible

579   for such crystallization (e.g., Buckley, 1951; Saratovin, 1959; Hill and Wanklyn, 1968; Keezer et

580   al., 1968; Doherty, 1980). Changes in calcite crystal morphology, for example, have commonly

581   been linked to increasing Mg content of the parent fluid (Devery and Ehlmann, 1981; Fernández-

582   Díaz et al., 1996). Meldrum and Hyde (2001), based on laboratory experiments, argued that the

583   addition of Mg resulted in (1) a wider range of crystal morphologies, and (2) a change from

584   single crystals to crystallite aggregates. Specifically, they noted a sequence from rhombs to

585   elongate rhombs to dumbbells to intergrown spheres as the Mg content increased. The relative

586   importance of Mg content as opposed to organics or other variables in natural systems is,

587   however, difficult to untangle (Meldrum and Hyde, 2001). Although those experiments

588   illustrated the role that Mg may play in crystal morphogenesis, it is commonly difficult to

589   translate that into natural spring systems. In many thermal springs in the Kenyan Rift Valley

590   (e.g., Jones and Renaut, 1996a, their Table 1) and in the Yunnan Province of China (e.g., Jones

591   and Peng, 2015, their Table 1), for example, the Mg content of the spring water is significantly

592   lower than the Ca content. This must, however, be treated with some caution because there is no

593   guarantee that the aragonite and calcite in those springs formed from the present-day waters or

594   from water that had the same composition as the water today.

595   Irrespective of the details, there is ample evidence from experimental work and the analysis

596   of thermal spring precipitates throughout the world that non-equilibrium precipitation of

597   aragonite and calcite is common. This carries important implications for other analytical

598   techniques that are commonly used in the characterization and interpretation of these deposits.

599   The δ^{18}O and δ^{13}C of the carbonate are commonly used to gain insights into the conditions

600   that existed as precipitation of aragonite and/or calcite took place. Use of the δ^{18}O for

601   calculating the temperature of the parent water, however, assumes that precipitation was in

602   isotopic equilibrium with the water, irrespective of the equation that is used (Kele et al., 2015).

603   Although some studies have suggested that the rate of calcite precipitation may also affect the

604   the oxygen fractionation between and calcite and water (Dietzel et al., 2009; Day and Henderson,

605   2011; Gabitov et al., 2012), other studies have suggested that there is no clear correlation

606   between the two parameters (Kele et al., 2015). As yet, potential linkages between

607   calcite/aragonite isotope values and crystal morphology have not been evaluated. If the crystal

608   morphology is characteristic of far-from-equilibrium conditions, then there is the possibility that

609   any temperature derived from the isotope will be invalid. This, however, can be difficult to

610   determine, especially given that the temperature of spring waters ranges from 0 to 100°C. In

611   some situations, the calculated temperatures are outside of this range and thus attest to non-

612   equilibrium precipitation (e.g., Jones and Peng, 2012). In other examples, however, the

613   calculated temperature falls within the 0 to 100°C range even though the crystal morphology

614   indicates non-equilibrium precipitation (e.g., Jones and Peng, 2016b, 2016a).

615   Data from laboratory experiments and thermal spring deposits clearly demonstrate that

616   aragonite and calcite crystal morphogenesis is extremely complex because it is controlled by

617   many different parameters that are commonly interlinked with each other. Although general

618   schemes like those proposed by Sunagawa (1981, 1982), Jones and Renaut (1995), and Oaki and

619   Imai (2003) provide some guidelines regarding crystal morphogenesis, it has so far proved

620   almost impossible to link specific crystal types with specific environmental parameters.

621   With our present knowledge of aragonite and calcite crystals morphogenesis it is usually

622   possible to provide a general idea of the conditions that led to growth of particular crystal

623   morphologies. Dendrites, for example, are usually indicative of non-equilibrium conditions.

624   Nevertheless, despite the numerous studies of natural spring systems and innumerable laboratory

625   experiments it remains impossible to precisely define the exact conditions that leads to the

626   precipitation of each type of crystal. This situation exists because it has proven impossible to

627   disentangle the complicated arrays of externally imposed physiochemical parameters that may, in

628   many situations, be further influenced by the microbes that thrive in these spring systems. Even

629   with laboratory experimental systems, which are far less complex than natural spring systems, it

630   is commonly difficult to exactly pinpoint the prime factor that is controlling $CaCO_3$ precipitation

631   and crystal morphogenesis. Future resolution of this problem may come from integration of

632   information from detailed analyses of natural spring systems and laboratory experiments. In

633   each setting, scale is a major problem because much of the precipitation in spring systems is

634   controlled by microscale processes that are extremely difficult to monitor with precision. In

635   addition, the precise roles that microbes play in the $CaCO_3$ precipitation in natural spring

636   systems also needs precise and careful evaluation.

637   **9. Conclusions**

638   The aragonite and calcite crystals that grow in thermal spring systems commonly develop

639   through non-classical crystal growth models that are, in some cases, mediated by the microbial

640   biofilms that thrive in these systems. Although laboratory experiments provide valuable insights

641   into the parameters that control aragonite and calcite crystal morphogenesis, it is commonly

642   difficult to apply those experimental results to natural thermal spring systems. Equally, however,

643   it is difficult to determine the underlying causes of crystal morphogenesis in natural systems

644   because of the problems associated with monitoring those systems and then disentangling the

645   parameters responsible for the precipitation of the aragonite and calcite crystals. Nevertheless,

646   the information that is presently available does allow evaluation of these crystalline precipitates

647   in terms of "the driving force", which is a conceptual measure that reflects all of the parameters

648   that control precipitation. Many crystals in thermal spring systems are precipitated under non-

649   equilibrium conditions, a fact that must be recognized in the interpretation of other analytical

650   data, including stable isotopes.

651   It is readily apparent from this review that much remains to be learnt about aragonite and

652   calcite crystal morphogenesis in thermal spring systems. Moving forward, the challenge is to

653   develop (1) field techniques that will allow detailed *in-situ* monitoring of these systems at all

654   scales, (2) laboratory experiments that are realistic in terms of thermal spring settings so that the

655   specific role that each parameter (e.g., water temperature, pH) plays in crystal growth can be

656   determined, and (3) a better understanding of the processes that mediate the precipitation of

657   aragonite and calcite crystals in the microbial biofilms. Integration of data from all of these

658   perspectives should provide a clearer understanding of the role(s) that each environmental

659   parameter plays in aragonite and calcite crystal morphogenesis.

REFERENCES

668

669

670 Albeck, S., Weiner, S., Addadi, L., 1996. Polysaccharides of intracrystalline glycoproteins

671   modulate calcite crystal growth in vitro. Chemistry European Journal 2, 278-284.

672 Alena, T., Hallett, J., Saunders, C.P.R., 1990. On the facet-skeletal transition of snow crystals:

673   experiments in high and low gravity. Journal of Crystal Growth 104, 539-555.

674 Asenath-Smith, E., Li, H., Keene, E.C., Seh, Z.W., Estroff, L.A., 2012. Crystal growth of

675   calcium carbonate in hydrogels as a model of biomineralization. Advanced Functional

676   Materials 22, 2891-2914.

677 Atanassova, R., Bonev, I.K., 2006. Two crystallographically different types of skeletal galena

678   associated with colloform sphalerite. Geochemistry, Mineralogy and Petrology 44, 1-18.

679 Beck, R., Andreassen, J.P., 2010. Spherulitic growth of calcium carbonate. Crystal Growth and

680   Design 10, 2934-2947.

681 Belcher, A.M., Wu, X.H., Christensen, R.J., Hansma, P.K., Stucky, G.D., Morse, D.E., 1996.

682   Control of crystal phase switching and orientation by soluble mollusc-shell proteins. Nature

683   381, 56-58.

684 Bergström, L., Sturm, E.V., Salazar-Alvarez., G., Cölfen, H., 2015. Mesocrystals in biominerals

685   and colloid arrays. Accounts of Chemical Research 48, 1391-14092.

686 Binkley, K.L., Wilkinson, B.H., Owen, R.M., 1980. Vadose beachrock cementation along a

687   southeastern Michigan marl lake. Journal of Sedimentary Petrology 50, 953-962.

688 Buckley, H.E., 1951. Crystal Growth. John Wiley and Sons Inc., London, 359 pp.

689 Buczynski, C., Chafetz, H.C., 1991. Habit of bacterially induced precipitates of calcium

690   carbonate and the influence of medium viscosity on mineralogy. Journal of Sedimentary

691   Petrology 61, 221-233.

692   Cady, S.L., Farmer, J.D., 1996. Fossilization processes in siliceous thermal springs: trends in

693   preservation along thermal gradients. In: Bock, G.R., Goode, J.A. (Eds.), Evolution of

694   Hydrothermal Ecosystems on Earth (and Mars?). Ciba Foundation Symposium. Wiley,

695   Chichester, U.K., pp. 150-173.

696   Chafetz, H.S., Rush, P.F., Utech, N.M., 1991. Microenvironmental controls on mineralogy and

697   habit of $CaCO_3$ precipitates: an example from an active travertine system. Sedimentology 38,

698   107-126.

699   Chafetz, H.S., Wilkinson, B.H., Love, K.M., 1985. Morphology and composition of non-marine

700   carbonate cements in near-surface settings. In: Schneidermann, N., Harris, P.M. (Eds.),

701   Carbonate Cements. Society of Economic Paleontologists and Mineralogists, Special

702   Publication 36, pp. 337-347.

703   Chalmers, B., 1964. Principles of Solidification. Wiley, New York, USA, 336 pp.

704   Chekroun, K.B., Rodrígues-Navarro, C., González-Muñoz, M.T., Arias, J.M., Cultrone, G.,

705   Rodríguez-Gallego, M., 2004. Precipitation and growth morphology of calcium carbonate

706   induced by *Myxococcus xanthus:* Implications for recognition of bacterial carbonates.

707   Journal of Sedimentary Research 74, 868-876.

708   Cölfen, H., Antonietti, M., 2005. Mesocrystals: Inorganic superstructures made by highly

709   parallel crystallization and controlled alignment. Angewandte Chemie 44, 5576-5591.

710   Coppens, P., Maly, K., Petricek, V., 1990. Composite crystals: What are they and why are they

711   so common in organic solid state? Molecular Crystals and Liquid Crystals Incorporating

712   Nonlinear Optics 181, 81-90.

713   Darling, W.G., Griesshaber, E., Andrews, J.N., Armannsson, H., O'Nions, R.K., 1995. The origin

714   of hydrothermal and other gases in the Kenya Rift Valley. Geochimica et Cosmochimica

715   Acta 59, 2501-2512.

716   Darwin, C.G., 1922. The reflection of X-rays from imperfect crystals. Philosopical Magazine

717   Series 6 43, 800-829.

718   Day, C.C., Henderson, G.M., 2011. Oxygen isotopes in calcite grown under cave-analogue

719   conditions. Geochimica et Cosmochimica Acta 75, 3956-3972.

720   Desiraju, G.R., 2003. Crystal and co-crystal. CrystEngComm 5, 466-467.

721   Devery, D.M., Ehlmann, A.J., 1981. Morphological changes in a series of synthetic Mg-calcites.

722   American Mineralogist 66, 592-595.

723   Dietzel, M., Tang, J., Leis, A., Köhler, S.J., 2009. Oxygen isotopic fractionation during inorganic

724   calcite precipitation – effects of temperature, precipitaiton rate, and pH. Chemical Geology

725   268, 107-115.

726   Doherty, R.D., 1980. Dendritic growth. In: Pamplin, B.R. (Ed.), Crystal Growth. Pergamon

727   Press, New York, pp. 485-520.

728   Dominguez Bella, S., Garcia-Ruiz, J.M., 1987. Banding structures in induced morphology

729   crystal aggregates of $CaCO_3$. Journal of Materials Science 22, 3095-3102.

730   Dorvee, J.R., Boskey, A.L., Estroff, L.A., 2012. Rediscovering hydrogel-based double diffusion

731   systems for studying biomineralization. CrystEngComm 14, 5681-5700.

732   Du, J., Liu, C., Fu, B., Ninomia, Y., Zhang, Y., Wang, C., Wang, H., Sun, Z., 2005. Variations of

733   geothermometry and chemical-isotope compositions of hot spring fluids in the Rehai

734   geothermal field, southwestern China. Journal of Volcanology and Geothermal Research

735   142, 243-261.

736 Fernández-Díaz, L., Putnis, A., Prieto, M., Putnis, C.V., 1996. The role of magnesium in the

737   crystallization of calcite and aragonite in porous medium. Journal of Sedimentary Research

738   66, 482-491.

739 Fisher, L.W., Simons, F.L., 1926. Applications of colloid chemistry to Mineralogy: Part I.

740   Preliminary Report. The American Mineralogist 11, 124-130.

741 Folk, R.L., 1993. SEM imaging of bacteria and nannobacteria in carbonate sediments and rocks.

742   Journal of Sedimentary Petrology 63, 990-999.

743 Folk, R.L., 1994. Interaction between bacteria, nannobacteria, and mineral precipitation in hot

744   springs of central Italy. Géographie physique et Quaternaire 48, 233-246.

745 Folk, R.L., Chafetz, H.S., Tiezzi, P.A., 1985. Bizarre forms of depositional and diagnetic calcite

746   in hot-spring travertines, central Italy. In: Schneidermann, N., Harris, P.M. (Eds.), Carbonate

747   Cements. Society of Economic Paleontologists and Mineralogists Special Publication No.

748   36, Tulsa, OK. pp. 349-369.

749 Fouke, B.W., Farmer, J.D., Des Marais, D.J., Pratt, L., Sturchio, N.C., Burns, P.C., Discipulo,

750   M.K., 2000. Depositional facies and aqueous-solid geochemistry of travertine-depositing hot

751   springs (Angel Terrace, Mammoth Hot Springs, Yellowstone National Park, USA). Journal

752   of Sedimentary Research 70, 565-585.

753 Francis, S., Margulis, L., Barghoorn, E.S., 1978. On the experimental silicification of

754   microorganisms. II. On the time of appearance of eukaryotic organisms in the fossil record.

755   Precambrian Research 6, 65-100.

756 French, B.M., Koeberl, C., 2010. The convincing identification of terrestrial meteorite impact

757   structures: What works, what doesn't, and why. Earth-Science Reviews 98, 123-170.

758   Gabitov, R.I., Watson, E.B., Sadekov, A., 2012. Oxygen isotope fractionation between calcite

759   and fluid as a function of growth rate and temperature. Chemical Geology 306-307, 92-102.

760   Garcia-Ruiz, J.M., 1985. On the formation of induced morphology crystal aggregates. Journal of

761   Crystal Growth 73, 251-262.

762   Gehrke, N., Cölfen, H., Pinna, N., Antonietti, M., Nassif, N., 2005. Superstructures of calcium

763   carbonate crystals by oriented attachment. Crystal Growth and Design 5, 1317-1319.

764   Geng, X., Liu, L., Jiang, J., Yu, S.-H., 2010. Crystallization of $CaCO_3$ mesocrystals and complex

765   aggregates in a mixed solvent media using polystyrene sulfonate as a crystal growth

766   modifier. Crystal Growth and Design 10, 3448-3453.

767   Given, R.K., Wilkinson, B.H., 1985. Kinetic control of morphology, composition and

768   mineralogy of abiotic sedimentary carbonates. Journal of Sedimentary Petrology 55, 109-

769   119.

770   Gornitz, V.M., Schreiber, B.H., 1981. Displacive halite hoppers from the Dead Sea: some

771   implications for ancient evaporative deposits. Journal of Sedimentary Petrology 62, 382-399.

772   Gránásy, L., Pusztai, G., Warren, J.A., Douglas, J.F., 2005. Growth and form of spherulites.

773   Physical Review E 72, 011605-1 to 011605-15.

774   Guo, L., Riding, R., 1992. Aragonite laminae in hot water travertine crusts, Rapolano Terme,

775   Italy. Sedimentology 39, 1067-1079.

776   Helbig, U., 2008. Growth of calcium carbonate in polyacrylamide hydrogel: Investigation of the

777   influence of polymer content. Journal of Crystal Growth 310, 2863-2870.

778   Herbstein, F.H., 2003. 5-Oxatricyclo[5.1.0.0^{1,3}]octan-4-one, containing an enantiomorph and a

779   racemate and not two polymorphs, is another example of a composite crystal. Acta

780   Crystallographica Section B59, 303-304.

781   Hill, G.J., Wanklyn, B.M., 1968. Fluxed-melt growth of nickel oxide crystals and their electrical

782   properties. Journal of Crystal Growth 3, 475-479.

783   Hörz, F., Quaide, W.L., 1973. Debye-Scherrer investigations of experimentally shocked silicates.

784   The Moon 6, 45-82.

785   Imai, H., 2014. Mesocrystals and their related structures as intermediates between single crsytals

786   and polycrystals. Journal of the Ceramic Society of Japan 122, 737-747.

787   Imai, H., 2016. Mesostructured crystals: Growth processes and features. Progress in Crystal

788   Growth and Characterization of Materials 62, 212-226.

789   Imai, H., Oaki, Y., 2010. Bioinspired hierarchial crystals. Materials Research Society Bulletin

790   35, 138-144.

791   Imai, H., Oaki, Y., Kotachi, A., 2006. A biomimetic approach for hierarchially structured

792   inorganic crystals through self-organization. Bulletin Chemical Society of Japan 79, 1834-

793   1851.

794   Inumaru, K., 2006. "Sponge Crystal": a novel class of microporous single crystals formed of

795   self-assembly of polyoxometalate $(NH_4)_3PW_{12}O_{40}$ nanocrystallites. Catalysis Surveys from

796   Asia 10, 151-160.

797   Jones, B., 1989. Syntaxial overgrowths on dolomite crystals in the Bluff Formation, Grand

798   Cayman, British West Indies. Journal of Sedimentary Petrology 59, 839-847.

799   Jones, B., 2017. Review of calcium carbonate polymorph precipitation in spring systems.

800   Sedimentary Geology.

801   Jones, B., Peng, X., 2012. Intrinsic versus extrinsic controls on the development of calcite

802   dendrite bushes, Shuzhishi Spring, Rehai geothermal area, Tengchong, Yunnan Province,

803   China. Sedimentary Geology 249-250, 45-62.

804   Jones, B., Peng, X., 2014a. Hot spring deposits on a cliff face: A case study from Jifei, Yunnan

805   Province, China. Sedimentary Geology 302, 1-28.

806   Jones, B., Peng, X., 2014b. Multiphase calcification associated with the atmophytic

807   cyanobacterium *Scytonema julianum*. Sedimentary Geology 313, 91-104.

808   Jones, B., Peng, X., 2014c. Signatures of biologically influenced $CaCO_3$ and Mg-Fe silicate

809   precipitation in hot springs: Case study from the Ruidian geothermal area, Western Yunnan

810   Province, China. Sedimentology 61, 56-89.

811   Jones, B., Peng, X., 2015. Laminae development in opal-A precipitates associated with seasonal

812   growth of the form-genus *Calothrix* (Cyanobacteria), Rehai geothermal area, Tengchong,

813   Yunnan Province, China. Sedimentary Geology 319, 52-68.

814   Jones, B., Peng, X., 2016a. Growth and development of spring towers at Shiqiang, Yunnan

815   Province, China. Sedimentary Geology 347, 183-209.

816   Jones, B., Peng, X., 2016b. Mineralogical, crystallographic, and isotopic constraints on the

817   precipitation of aragonite and calcite at Shiqiang and other hot springs in Yunnan Province,

818   China. Sedimentary Geology 345, 103-125.

819   Jones, B., Renaut, R.W., 1995. Noncrystallographic dendrites from hot-spring deposits at Lake

820   Bogoria, Kenya. Journal of Sedimentary Research A65, 154-169.

821   Jones, B., Renaut, R.W., 1996a. Morphology and growth of aragonite crystals in hot-spring

822   travertines at Lake Bogoria, Kenya Rift Valley. Sedimentology 43, 323-340.

823   Jones, B., Renaut, R.W., 1996b. Skeletal crystals of calcite and trona from hot-spring deposits in

824   Kenya and New Zealand. Journal of Sedimentary Research 66, 265-274.

825   Jones, B., Renaut, R.W., 2008. Cyclic development of large, complex calcite dendrite crystals in

826   the Clinton travertine, Interior British Columbia, Canada. Sedimentary Geology 203, 17-35.

827   Jones, B., Renaut, R.W., Owen, R.B., Torfason, H., 2005. Growth patterns and implications of

828   complex dendrites in calcite travertines from Lýsuhóll, Snæfellsnes, Iceland. Sedimentology

829   52, 1277-1301.

830   Jones, B., Renaut, R.W., Rosen, M.R., 1998. Microbial biofacies in hot-spring sinters: A model

831   based on Ohaaki Pool, North Island, New Zealand. Journal of Sedimentary Research 68,

832   413-434.

833   Jones, B., Renaut, R.W., Rosen, M.R., 2000. Trigonal dendritic calcite crystals forming from hot

834   spring waters at Waikite, North Island, New Zealand. Journal of Sedimentary Research 70,

835   586-603.

836   Jones, B., Renaut, R.W., Rosen, M.R., 2003. Silicified microbes in a geyser mound: The enigma

837   of low-temperature cyanobacteria in a high-temperature setting. Palaios 18, 87-109.

838   Jones, B., Renaut, R.W., Rosen, M.R., 2004. Taxonomic fidelity of silicified microbes from hot

839   spring systems in the Taupo Volcanic Zone, North Island, New Zealand. Transactions of the

840   Royal Society of Edinburgh: Earth Sciences 94, 475-483.

841   Keezer, R.C., Griffiths, C.H., Vernon, J.P., 1968. Crystal-growth phenomena in the selenium-

842   tellurium system. Journal of Crystal Growth 3-4, 755-760.

843   Keith, H.D., Padden, F.J., 1964. Spherulitic crystallization from the melt. I. Fractionation and

844   impurity segregation and their influence on crystalline morphology. Journal of Applied

845   Physics 35, 1270-1285.

846   Kim, Y.-Y., Schenk, A.S., Ihli, J., Kulak, A.N., Hetherington, N.B.J., Tang, C.C., Schmahl,

847   W.W., Griesshaber, E., Hyett, G., Meldrum, F.C., 2014. A critical analysis of calcium

848   carbonate mesocrystals. Nature Communications 5, 1-14. DOI: 10.1038/ncomms5341.

849 Kitano, Y., 1962. A study of the polymorphic formation of calcium carbonate in thermal springs

850   with an emphasis of the effect of temperature. Journal of Earth Sciences, Nagoya University

851   35, 1980-1985.

852 Kele, S., Breitenbach, S.F.M., Capezzuoli, E., Meckler, A.N., Ziegler, M., Millan, I.M., Kluge,

853   T., Deák, J., Hanelmann, K., John, C.M., Yan, H., Liu, Z., Bernasconi, M., 2015.

854   Temperature dependence of oxygen- and clumped isotope fractionation in carbonates: A

855   study of travertines and tufas in the 6–96°C temperature range. Geochimica et Comochimica

856   Acta, 168, 172-192.

857 Konhauser, K.O., Phoenix, V.R., Bottrell, S.H., Adams, D.G., Head, I.M., 1999. Microbial-silica

858   interactions in modern hot spring sinter. In: Armannsson, H. (Ed.), Geochemistry of the

859   Earth's Surface. A.A. Balkema, Rotterdam, pp. 263-266.

860 Kulak, A.N., Iddon, P., Li, Y., Armes, S.P., Cölfen, H., Paris, O., Wilson, R.M., Meldrum, F.C.,

861   2007. Continuous structural evolution of calcium carbonate particles: A unifying model of

862   copolymer-mediated crystallization. Journal of the American Chemical Society 12, 3729-

863   2736.

864 Li, H., Estroff, L.A., 2007. Porous calcite single crystals grown in a hydrogel medium.

865   CrystEngComm 9, 1153-1155.

866 Lofgren, G., 1974. An experimental study of plagioclase crystal morphology: Isothermal

867   crystallization. American Journal of Science 274, 243-273.

868 Loste, E., Wilson, R.M., Seshadri, R., Meldrum, F.C., 2003. The role of magnesium in sabilizing

869   amorphous calcium carbonate and controlling calcite morphologies. Journal of Crystal

870   Growth 354, 206-218.

871 Lowenstam, H.A., Weiner, S., 1989. On Biomineralization. Oxford University Press, New York,

872   336 pp.

873 McCall, G.J.H., 1967. Geology of the Nakuru – Thomson's Falls – Lake Harrington area: Degree

874   sheet No. 35 SW Quarter and 43 NW Quarter (with coloured maps). Geological Survey of

875   Kenya, Report 78.

876 McCauley, J., Roy, R., 1974. Controlled nucleation and crystal growth of various $CaCO_3$ phases

877   by the silica gel technique. American Mineralogist 59, 947-963.

878 Meldrum, F.C., 2003. Calcium carbonate in biomineralisation and biomimetic chemistry.

879   International Materials Review 48, 187-224.

880 Meldrum, F.C., Cölfen, H., 2008. Controlling mineral morphologies and structures in biological

881   and synthetic systems. Chemical Reviews 108, 4332-4432.

882 Meldrum, F.C., Hyde, S.T., 2001. Morphological influence of magnesium and organic additives

883   on the precipitation of calcite. Journal of Crystal Growth 231, 544-558.

884 Niederberger, M., Cölfen, H., 2006. Oriented attachment and mesocrystals: Non-classical

885   crystallization mechanisms based on nanoparticle assembly. Physical Chemistry Chemical

886   Physics 8, 3271-3287.

887 Nindiyasari, F., Fernández-Díaz, L., Griesshaber, E., Astilleros, J.M., Sánchez-Pastor, N.,

888   Schmahl, W.W., 2014. Influence of gelatin hydrogel porosity on the crystallization of

889      $CaCO_3$. Crystal Growth and Design 14, 1531-1542.

890 Nindiyasari, F., Ziegler, A., Griesshaber, E., Fernández-Díaz, L., Huber, J., Walther, P.,

891   Schmahl, W.W., 2015. Effect of hydrogel matrices on calcite crystal growth morphology,

892   aggregate formation, and co-orientation in biomimetic experiments and biomineralization

893   environments. Crystal Growth and Design 15, 2667-2685.

894   Oaki, Y., Imai, Y., 2003. Experimental demonstration for the morphological evolution of crystals

895   grown in gel media. Crystal Growth and Design 3, 711-716.

896   Oehler, L.H., Schopf, J.W., 1971. Artificial microfossils: Experimental studies of

897   permineralization of blue-green algae in silica. Science 174, 1229-1231.

898   Okumura, T., Takashima, C., Shiraishi, F., Akmaluddin, Kano, A., 2012. Textural transition in

899   an aragonite travertine formed under various flow conditions at Pancuran Pitu, Central Java,

900   Indonesia. Sedimentary Geology 265-266, 195-209.

901   Okumura, T., Takashima, C., Shiraishi, F., Nishida, S., Yukimura, K., Naganuma, T., Arp, G.,

902   Kano, A., 2011. Microbial processes forming daily lamination in an aragonite travertine,

903   Nagano-yu Hot Spring, southwest Japan. Geomicrobiological Journal 28, 135-148.

904   Pedley, M., Rogerson, M., Middleton, R., 2009. Freshwater calcite precipitates from in vitro

905   mesocosm flume experiments: A case for biomediation of tufas. Sedimentology 56, 511-

906   527.

907   Peng, X., Jones, B., 2012. Rapid precipitation of silica (opal-A) disguises evidence of biogenicity

908   in high-temperature geothermal deposits: Case study from Dagunguo hot spring, China.

909   Sedimentary Geology 257-258, 45-62.

910   Peng, X., Jones, B., 2013. Patterns of biomediated $CaCO_3$ crystal bushes in hot spring deposits.

911   Sedimentary Geology 294, 105-117.

912   Penn, R.L., Banfield, J.F., 1998a. Imperfect oriented attachment: Dislocation generation in

913   defect-free nano crystals. Science 281, 969-971.

914   Penn, R.L., Banfield, J.F., 1998b. Oriented attachement and growth, twinning, polytypism, and

915   formation of metastable phases: Insights from nanocrytalline TiO_2. American Mineralogist

916   83, 1077-1082.

917　Penn, R.L., Banfield, J.F., 1999. Morphology development and crystal growth in nanocrystalline

918　　　aggregates under hydrothermal conditions: Insights from titania. Geochimica et

919　　　Cosmochimica Acta 63, 1549-1557.

920　Pentecost, A., 2005. Travertine. Springer, Berlin Heidelberg, 445 pp.

921　Rainey, D.K., Jones, B., 2007. Rapid cold water formation and recrystallization of relict

922　　　bryophyte tufa at the Fall Creek cold springs, Alberta, Canada. Canadian Journal of Earth

923　　　Sciences 44, 889-909.

924　Rainey, D.K., Jones, B., 2009. Abiotic versus biotic controls on the development of the Fairmont

925　　　hot Springs carbonate deposit, British Columbia, Canada. Sedimentology 56, 1832-1857.

926　Ramseier, R., 1967. Self-diffusion of tritium in natural and synthetic ice monocrystals. Journal of

927　　　Applied Physics 38, 3553-3556.

928　Reddy, M.M., Nancollas, G.H., 1976. The crystallization of calcium carbonate (IV. The effect of

929　　　magnesium, strontium, and sulfate ions). Journal of Crystal Growth 35, 33-38.

930　Reddy, M.M., Wang, K.K., 1980. Crystallization of calcium carbonate in the presence of metal

931　　　ions. I. Inhibition by magnesium ion at pH 8.8 and 25°C. Journal of Crystal Growth 50, 470-

932　　　480.

933　Ren, J., Wang, X., Ouyang, Z., 2005. Mantle-derived CO_2 in hot springs of the Rehai geothermal

934　　　field, Tengchong, China. Acta Geologica Sinica 79, 426-431.

935　Renaut, R.W., Jones, B., 1997. Controls on aragonite and calcite precipitation in hot spring

936　　　travertines at Chemurkeu, Lake Bogoria, Kenya. Canadian Journal of Earth Sciences 34,

937　　　801-814.

938　Renaut, R.W., Jones, B., Tiercelin, J.-J., 1998. Rapid *in situ* silicification of microbes at Loburu

939　　　hot springs, Lake Bogoria, Kenya Rift Valley. Sedimentology 45, 1083-1103.

940   Rogerson, M., Pedley, H.M., Wadhawan, J.D., Middleton, R., 2008. New insights into biological

941   influence on the geochemistry of freshwater carbonate deposits. Geochimica et

942   Cosmochimica Acta 72, 4976-4987.

943   Ruiz-Agudi, E., Putnis, C.V., Rodriguez-Navarro, C., Putnis, A., 2011. Effect of pH on calcite

944   growth at constant $a_{Ca^{2+}}/a_{CO_3^{2-}}$ ratio and supesaturation. Geochimica et Cosmochimica Acta

945   75, 284-296.

946   Sánchez-Pastor, N., Gigler, A.M., Cruz, J.A., Park, S.H., Jordan, G., Fernández-Díaz, L., 2011.

947   Growth of calcium carbonate in the presence of Cr(VI). Crystal Growth and Design 11,

948   3081-3089.

949   Sand, K.K., Rodriguez-Blanco, J.D., Makovicky, E., Benning, L.G., Stipp, S.L.S., 2012.

950   Crystallization of $CaCO_3$ in water-alcohol mixtures: Spherulitic growth, polymorph

951   stabilization, and morphology change. Crystal Growth and Design 12, 842-853.

952   Sandberg, P., 1985. Aragonite cements and their occurrence in ancient limestones. In:

953   Schneidermann, N., Harris, P.M. (Eds.), Carbonate Cements. Society of Economic

954   Paleontologists and Mineralogists Special Publication No. 36, pp. 33-57.

955   Saratovin, D.D., 1959. Dendritic Crystallization. Consultants Bureau, Inc., New York, pp. 20-70.

956   Seto, J., Ma, Y., Davis, S.A., Meldrum, F.C., Gourrier, A., Kim, Y.K., Schilde, U., Sztucki, M.,

957   Burghammer, M., Maltsev, S., Jäger, C., Cölfen, H., 2012. Structure-property relationships

958   of a biological mesocrystal in the adult sea urchin spine. Proceedings of National Academy

959   of Science, USA 109, 3699-3704.

960   Shangguan, Z., Zhao, C., Li, H., Gao, Q., Sun, M., 2005. Evolution of hydrothermal explosions

961   at Rehai geothermal field, Tengchong volcanic region, China. Geothermics 34, 58-526.

962   Smith, C.S., 1965. A History of Metallography. The Development of Ideas on the Structure of

963   Metals Before 1890. University of Chicargo Press, Chicago, USA, 326 pp.

964   Song, R.-Q., Cölfen, H., 2010. Mesocrystals – ordered nanoparticle superstructures. Advanced

965   Materials 22, 1301-1330.

966   Song, R.-Q., Cölfen, H., 2011. Additive controlled crysallization. CrystEngComm 13, 1249-

967   1276.

968   Song, R.-Q., Xu, A.W., Antonietti, M., Cölfen, H., 2009. Calcite crystals with platonic shapes

969   and minimal surfaces. Angewandte Chemie 48, 395-399.

970   Southgate, P.N., 1982. Cambrian skeletal halite crystals and experimental analogues.

971   Sedimentology 29, 391-407.

972   Strickland-Constable, R.F., 1968. Kinetics and mechanism of crystallization. Academic Press,

973   London, New York, 347 pp.

974   Sunagawa, I., 1981. Characteristics of crystal growth in nature as seen from the morphology of

975   mineral crystals. Bulletin Mineralogie 104, 81-87.

976   Sunagawa, I., 1982. Morphology of crystals in relation to growth conditions. Estudios

977   Geologicos 38, 127-134.

978   Sunagawa, I., 2005. Crystals: Growth, Morphology and Perfection. Cambridge University Press,

979   Cambridge, 308 pp.

980   Taylor, P.M., Chafetz, H.S., 2004. Floating rafts of calcite crystals in cave pools, central Texas,

981   U.S.A.: Crystal habit vs. saturation state. Journal of Sedimentary Research 74, 328-341.

982   Torrent-Burgésm J., 1994. The Gibbs energy and the driving force at crystallization from

983   solution. Journal of Crystal Growth 140, 107-114.

984   Thattey, A.S., Risbud, S., 1969. On the growth of zinc monocrystals from the vapor phase.

985   Current Science 38, 405-406.

986   Turner, E.C., Jones, B., 2005. Microscopic calcite dendrites in cold-water tufa: Implications for

987   nucleation of micrite and cement. Sedimentology 52, 1043-1066.

988   Van der Weijden, C.H., Van der Weijden, R.D., 2014. Calcite growth: Rate dependence on

989   saturation, on ratios of dissolved calcium and (bi)carbonate and on their complexes. Journal

990   of Crysal Growth 394, 137-144.

991   Wang, Y.Y., Yao, Q.Z., Zhou, G.T., Fu, S.Q., 2013. Formation of elongated calcite mesocrsytals

992   and implication for biomineralization. Chemical Geology 360-361, 126-133.

993   Waring, G.A., 1965. Thermal springs of the United States and other countries of the world – A

994   summary. United States Geological Survey Professional Paper 492, 383 pp.

995   Wasylenki, L.E., Dove, P.M., De Yoreo, J.J., 2005. Effects of temperature and transport

996   conditions on calcite growth in the presence of Mg^{2+}: Implications for paleothermometry.

997   Geochimica et Cosmochimica Acta 69, 4227-4236.

998   Wells, A.K., Bishop, A.C., 1955. An appinitic facies associated with certain granites in Jersey,

999   Channel Islands. Quarterly Journal of the Geological Society of London 111, 143-166.

1000   Westall, F., Boni, L., Guerzoni, E., 1995. The experimental silicification of microorganisms.

1001   Palaeontology 38, 495-528.

1002   Xu, A.W., Antonietti, M., Cölfen, H., Fang, Y.P., 2006. Uniform hexagonal plates of vaterite

1003 $CaCO_3$ mesocrystals formed by biomimetic mineralization. Advanced Functional Materials

1004   16, 903-908.

1005 Xu, A.W., Antonietti, M., Yu, S.H., Cölfen, H., 2008a. Polymer-mediated mineralization and

1006   self-similar mesoscale-organized calcium carbonate with unusual superstructures. Advanced

1007   Materials 20, 1333-1338.

1008 Xu, X., Cai, A., Liu, R., Pan, H., Tang, R., Cho, K., 2008b. The roles of water and

1009   polyelectrolytes in the phase transformation of amorphous calcium carbonate. Journal of

1010   Crystal Growth 310, 3779-3787.

1011 Zhan, J., Lin, H.P., Mou, C.Y., 2003. Biomimetic formation of porous single-crystalline $CaCO_3$

1012   via nanocrystal aggregation. Advanced Materials 15, 621-623.

1013 Zhang, J., Huang, F., lin, Z., 2010. Progress of nanocrystalline growth kinetics based on oreinted

1014   attachment. Nanoscale 2, 18-34.

1015 Zhou, G.-T., Yao, Q.-Z., Ni, J., Jin, G., 2009. Formation of aragonite mesocrystals and

1016   implications for biomineralization. American Mineralogist 94, 293-302.

1017 Zhou, G.T., Guan, Y.B., Yao, Q.Z., Fu, S.Q., 2010. Biomimetic mineralization of prismatic

1018   calcite mesocrystals: Relevance to biomineralization. Chemical Geology 279, 63-72.

1019 Zhou, L.P., O'Brien, P., 2008. Mesocrystals: A new class of solid materials. Small 4, 1566-1574.

1020 Zhou, L.P., O'Brien, P., 2012. Mesocrystals – properties and applications. The Journal of

1021   Physical Chemistry Letters 3, 620-628.

1022

48

FIGURE CAPTIONS

1023

1024   **Fig. 1.** Relationship between crystal morphology and driving force (see text for explanation).

1025   Adapted from Jones and Renaut (1995, their Fig. 14) with monocrystals added herein. P =

1026   pore; NC = nanocrystal; arrows on nanocrystals indicate growth axis.

1027   **Fig. 2.** Examples of aragonite crystals from spring deposits found at (A) LaXin (see Jones and

1028   Peng, 2014c, for detailed information), (B) Jifei (see Jones and Peng, 2014a, for detailed

1029   information), and (C, D) Eryuan hot springs (see Peng and Jones, 2013, for detailed

1030   information), Yunnan Province, China. (A) Group of hexagonal aragonite crystals, with

1031   each crystal face having a zig-zag suture line (arrows) that is indicative of cyclic twinning.

1032   (B) Bushes formed of nested splays of radiating aragonite crystals. This is not a dendrite

1033   because each branch is a separate cyclically twinned crystal. (C) Dumbbell formed of

1034   aragonite crystals. (D) Spherulitic growth of aragonite crystals.

1035   **Fig. 3.** Calcite mesocrystals from unnamed spring at Lýsuhóll, Iceland. Sample ~ 6 m from

1036   spring vent, water temperature of 16°C. (A) Large, mesocrystal formed of numerous thin,

1037   rhombic nanocrystals that all have a common orientation. Note strands of EPS (arrow)

1038   spanning some of the larger gaps. (B) Enlarged view of nanocrystals that form the large

1039   mesocrystals shown in panel A. Each nanocrystal is formed of even smaller nanocrsytals.

1040   Note strands of EPS (arrows). (C-E) Individual nanocrystals, each formed of smaller

1041   nanocrystals, with consistent morphologies despite varying in size. Note associated EPS

1042   (arrows). (F) Group of prismatic calcite crystals and associated EPS (arrows). White letter

1043   G indicates position of panel G. (G) Face of prismatic crystal (from panel F) formed of

1044   stacked nanocrystals with common crystallographic orientations. (H, I) Enlarged views of

49

1045   nanocrystals from area shown in panel G. Note consistent orientation of the nanocrystals

1046   even though some are incompletely developed.

1047   **Fig. 4.** Dodecahedral mesocrystals from spring deposits on cliff face (A-C) and lining PVC pipe

1048   (D-F) at Jifei (see Jones and Peng, 2014a, for detailed information) and Gongxiaoshe,

1049   LaXin (see Jones and Peng, 2014c, for detailed information), Yunnan Province, China. (A)

1050   Unattached dodecahedral crystals of various sizes and shapes associated with filamentous

1051   microbes and ESP. (B, C) Incompletely formed dodecahedral crystals with poorly formed

1052   smooth crystal faces, missing or poorly developed crystal edges, and interiors formed of

1053   nanocrystals. (D) Incompletely formed, unattached dodecahedron crystal from precipitates

1054   lining interior of PVC pipe that formed within 6 months. Note variable development of

1055   crystal faces, edges, and nanocrystals. (E) Corner of dodecahedral crystal, from PVC pipe,

1056   showing smooth, poorly formed crystal faces, lack of crystal edges, and interior formed of

1057   nanocrystals. (F) Almost complete dodecahedral calcite crystal from PVC pipe. (G) Two

1058   interlocking, unattached and incompletely formed dodecahedrons with variable

1059   development of crystal faces and interiors formed of nanocrystals. (H) Dodecahedron

1060   mesocrystal with poorly developed crystal faces, no crystal edges, and interior formed of

1061   nanocrystals. (I) Enlarged view of lower left corner of crystal shown in panel H, showing

1062   nature of crystal faces and interior of crystal.

1063   **Fig. 5.** Examples of trigonal mesocrystals from (A-F) Waikite Spring in New Zealand (see Jones

1064   and Renaut, 1996b, for detailed information) and (G-I) Clinton spring, British Columbia,

1065   Canada (see Jones and Renaut, 2008, for detailed information). (A) Side of trigonal prism

1066   showing constituent nanocrystals. Note hollow core. (B, C) Views down c-axes of trigonal

1067   mesocrystals showing trigonal outlines of the constituent nanocrystals. (D) Skeletal trigonal

1068   crystal with walls formed of trigonal nanocrystals. (E) Enlarged view of upper left corner

1069   of trigonal crystal shown in panel D. Note common orientations of constituent

1070   nanocrystals. (F) View down wall of trigonal mesocrystals showing layer formed of

1071   trigonal nanocrystals with common crystallographic orientations. (G) Group of trigonal

1072   nanocrystals with common orientation. (H, I) Views down c-axes of trigonal mesocrystals

1073   showing constituent nanocrystals.

1074   **Fig. 6**. Scanning electron microscope photomicrographs showing general attributes of calcite

1075   dendrite crystals from (A, B) Clinton, Canada (see Jones and Renaut, 2008 for detailed

1076   information); (C, D) Tengchong, Yunnan Province, China (see Jones and Peng, 2012 for

1077   detailed information); and (E) Eryuan, Yunnan Province, China (see Peng and Jones, 2013

1078   for detailed information). (A) Cross-section through large dendrite crystal showing multiple

1079   levels of branching. Box labeled B indicates area shown in panel B. (B) Branches formed

1080   of stacked calcite crystals. (C, D) Complex calcite crystals with new branches developing

1081   through crystal splitting. (E) Calcite dendrite with branches developing from main branches

1082   (arrows).

1083   **Fig. 7.** Dendrites associated with modern spring at Lýsuhóll, Iceland. (A) Example of three-

1084   dimensional calcite dendrites growing in shallow pool on outflow apron of unnamed spring

1085   at Lysuholl. Although not evident in the photograph, the dendrites are coated with a thin

1086   layer of EPS. (B) Area of outflow apron, close to area shown in panel A, but with calcite

1087   precipitates largely obscured by actively growing microbial mat formed of filaments and

1088   EPS.

1089   **Fig. 8.** Diagram showing relationships between crystal morphology, driving force, and rate

1090   determining processes. Main part from Oaki and Imai (2003, their Fig. 1) is based on

1091   experimental laboratory precipitation of various types of crystals in different types of gels.

1092   The relationship between the density of gel matrix and crystal form is from Imai (2016, his

1093   Fig. 7).

1094

1095

Figure 1

MONOCRYSTAL
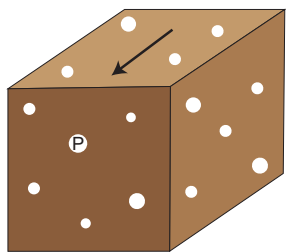
POLYCRYSTAL

DENDRITE CRYSTALS

Monocrystal
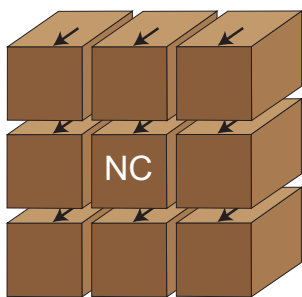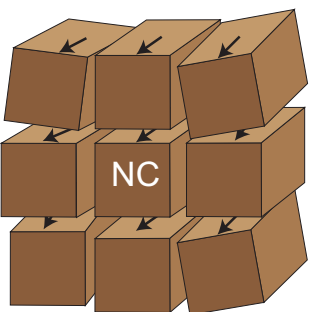
Porous monocrystal

SKELETAL CRYSTALS

No core

Skeletal crystal
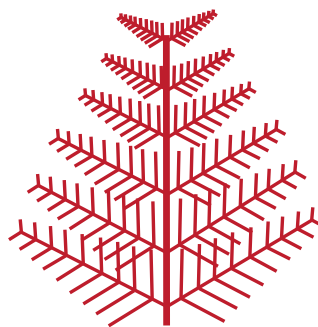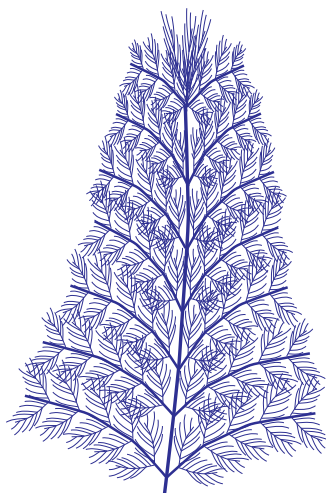
Crystallographic dendrite

SPHERULITIC CRYSTALS

Wheat sheaf

Mesocrystal

NC

NC

Mosaic crystal

Non-crystallographic dendrite
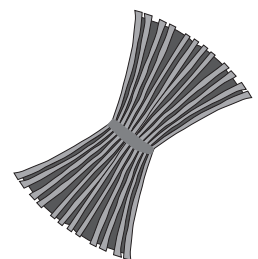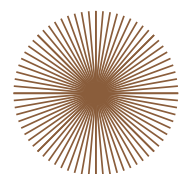
Sperulite

Driving force (supersaturation, supercooling)

Figure 2
Click here to download high resolution image
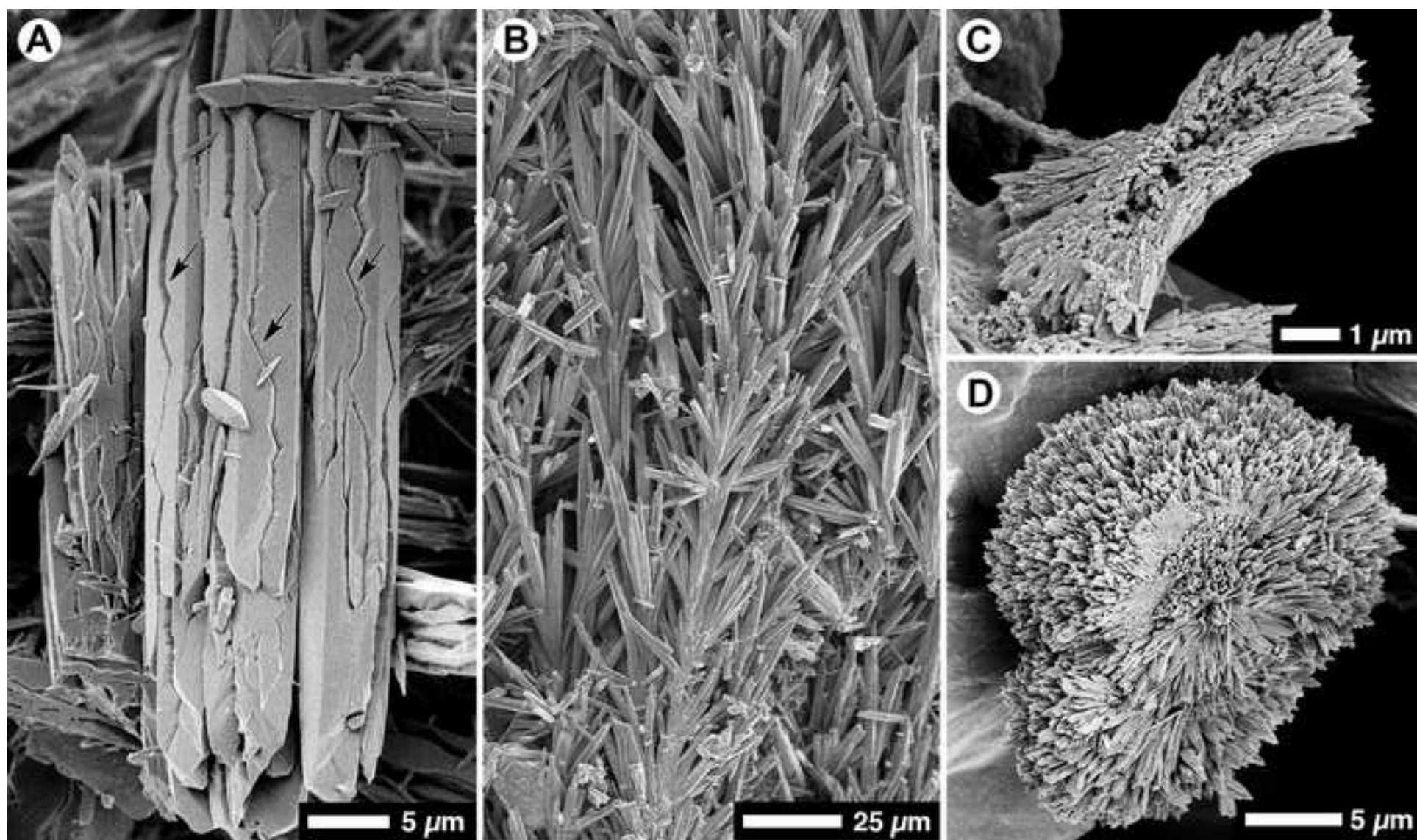
Figure 3
Click here to download high resolution image
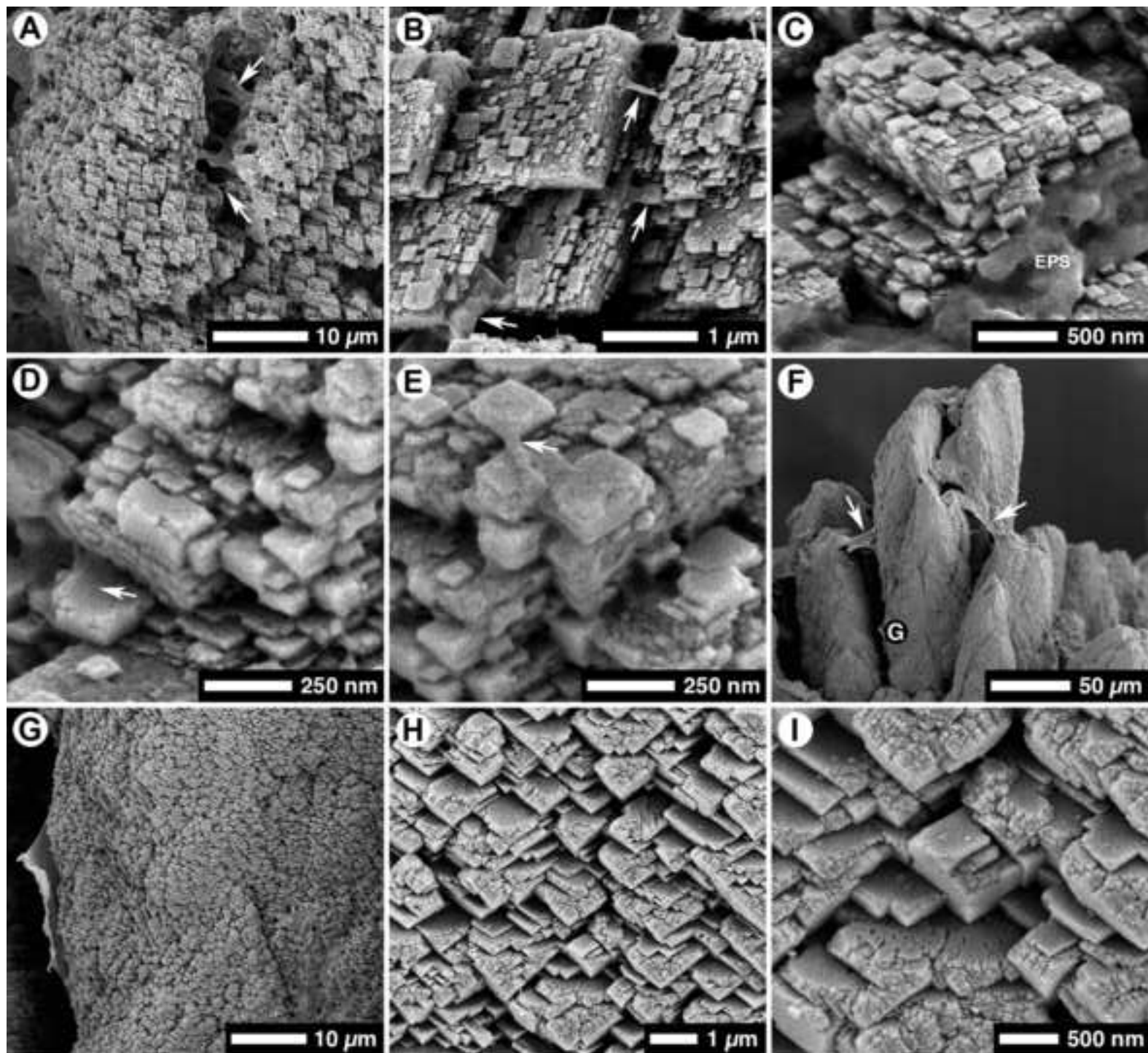
Figure 4
Click here to download high resolution image
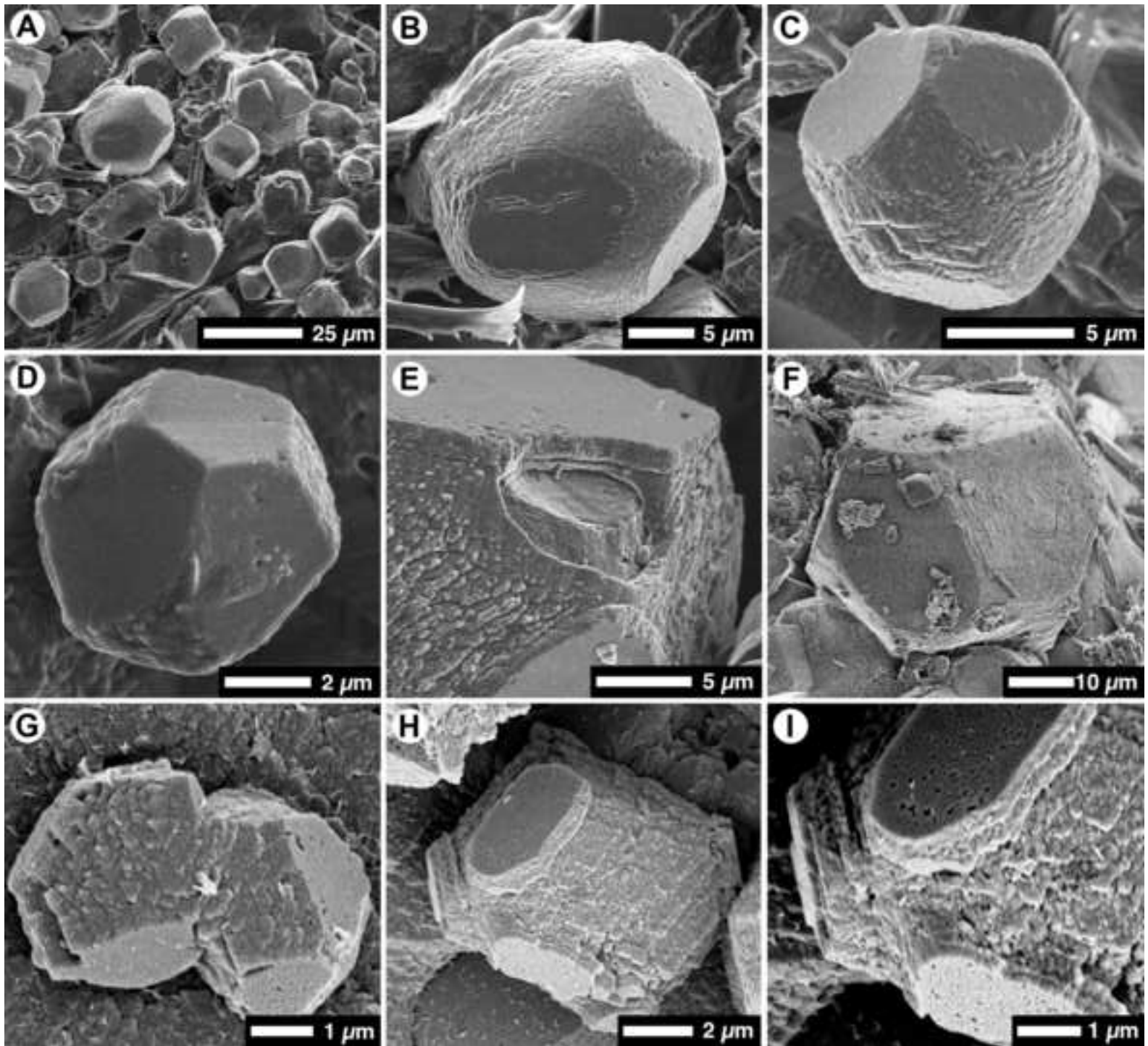
Figure 5
[Click here to download high resolution image](#)
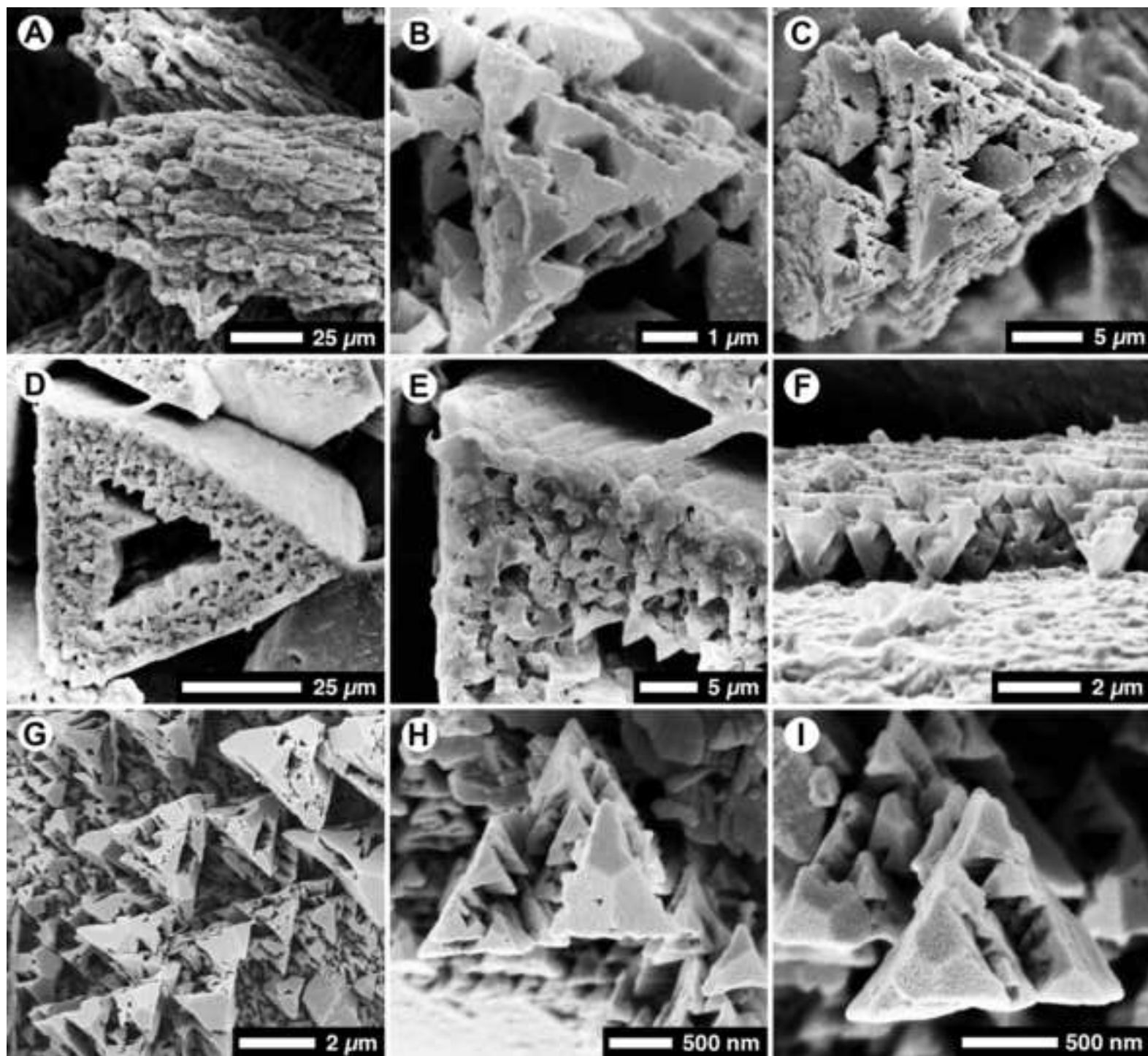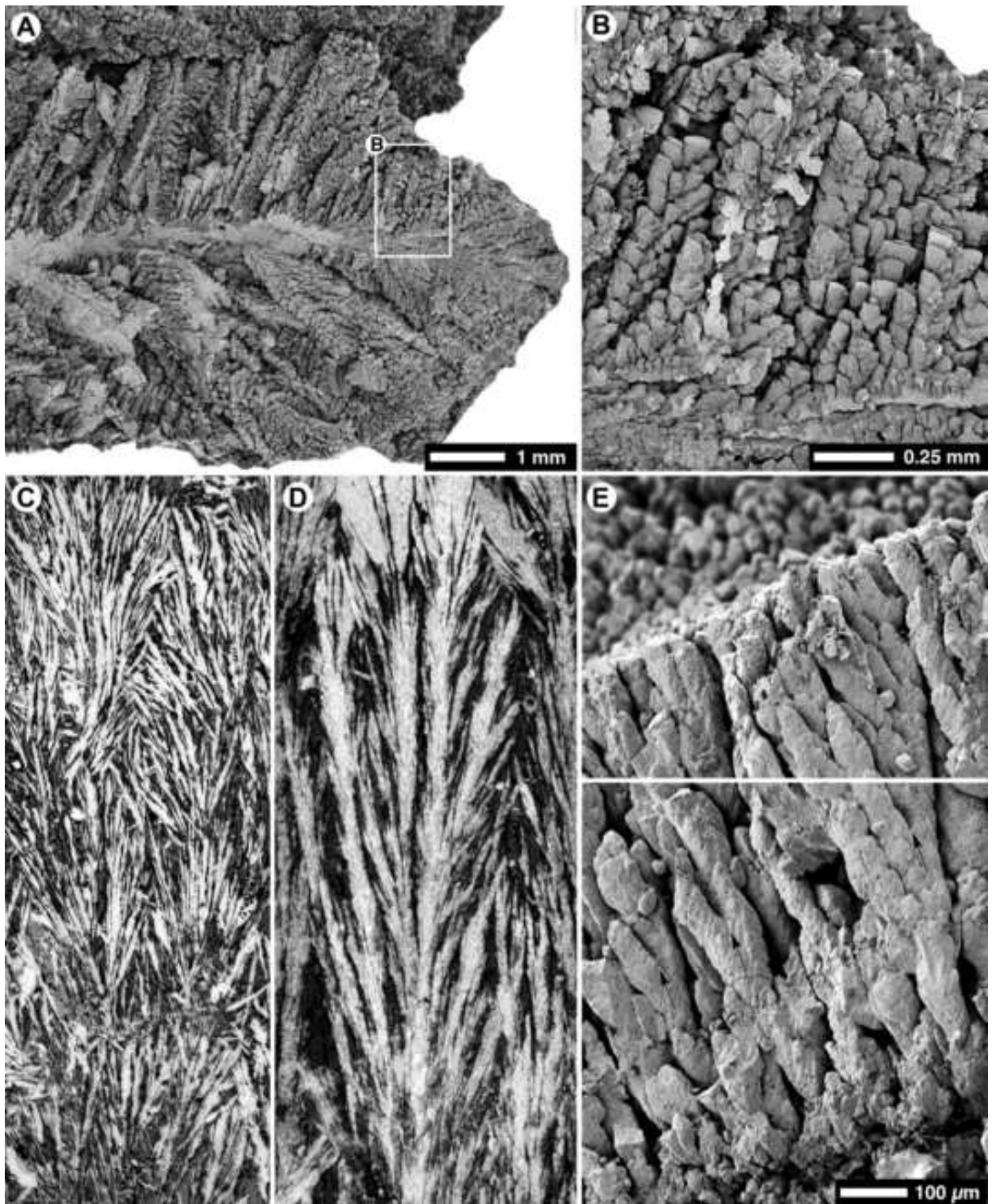
Figure 7
Click here to download high resolution image
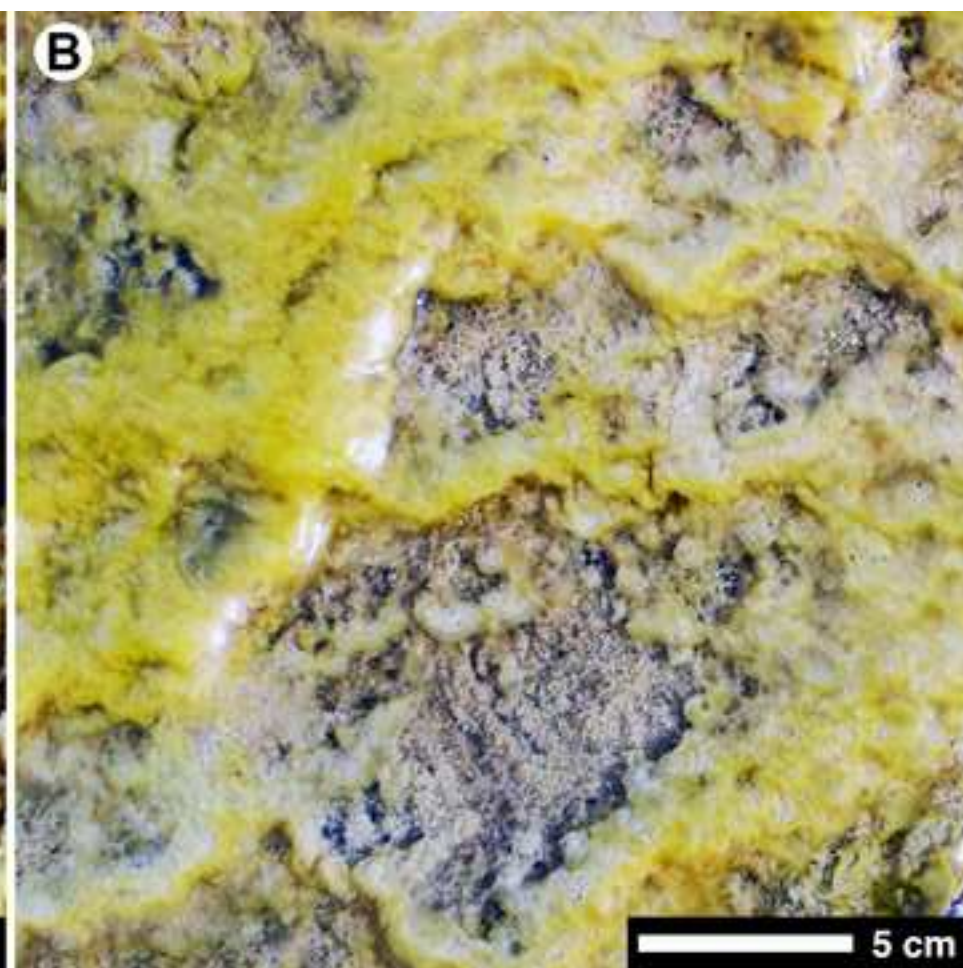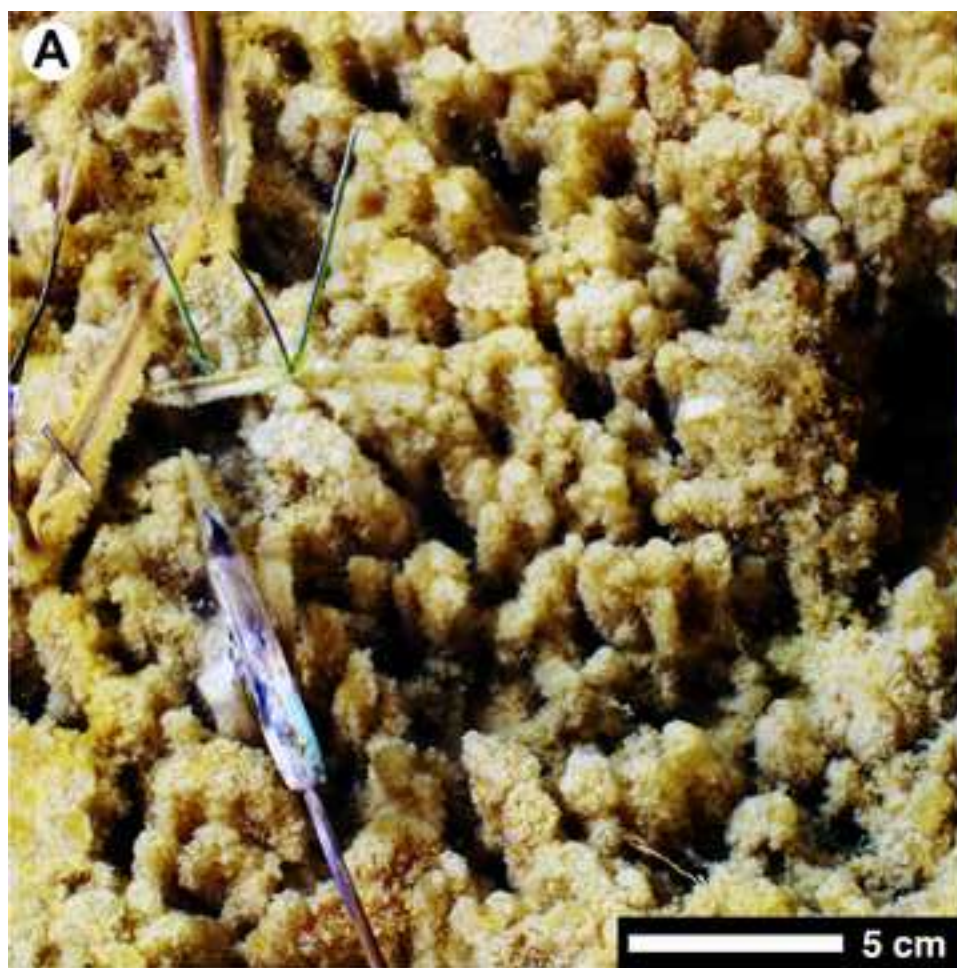
Figure 8

MORPHOLOGY

DRIVING FORCE (supersaturation, supercooling)

RATE DETERMINING
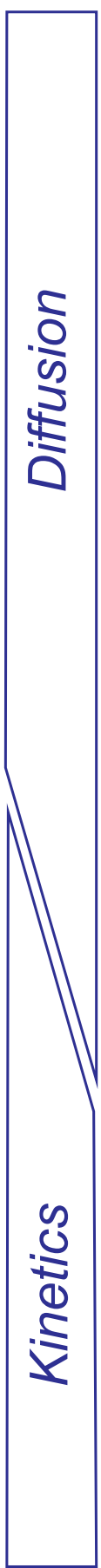
Diffusion

Density of gel matrix

Kinetics

Dense branching morphology
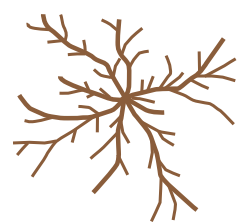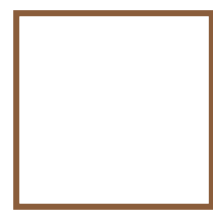
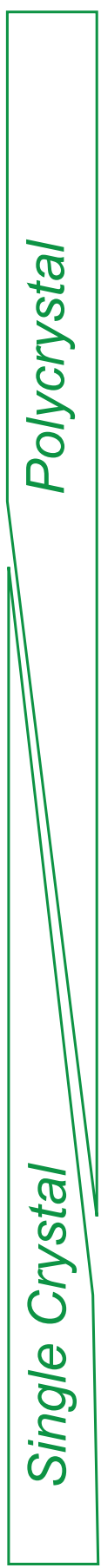*Disordered polycrystalline dendrite*
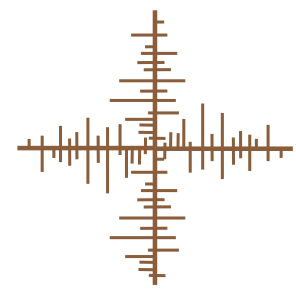
Partially disordered dendrite
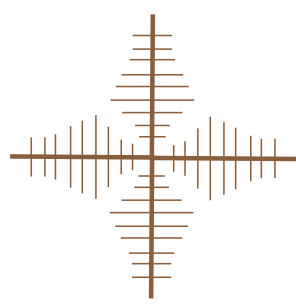
Single-crystal ordered dendrite with crystallographic symmetry
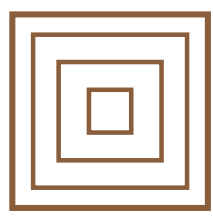
Skeletal

Polyhedral

Polycrystal

Single Crystal

CRYSTAL STRUCTURE